JULY 2025

Volume 2, Issue 6

NUCLEIC ACID INSIGHTS

CONTENT PILLAR

Formulation and Delivery

Getting beyond the liver

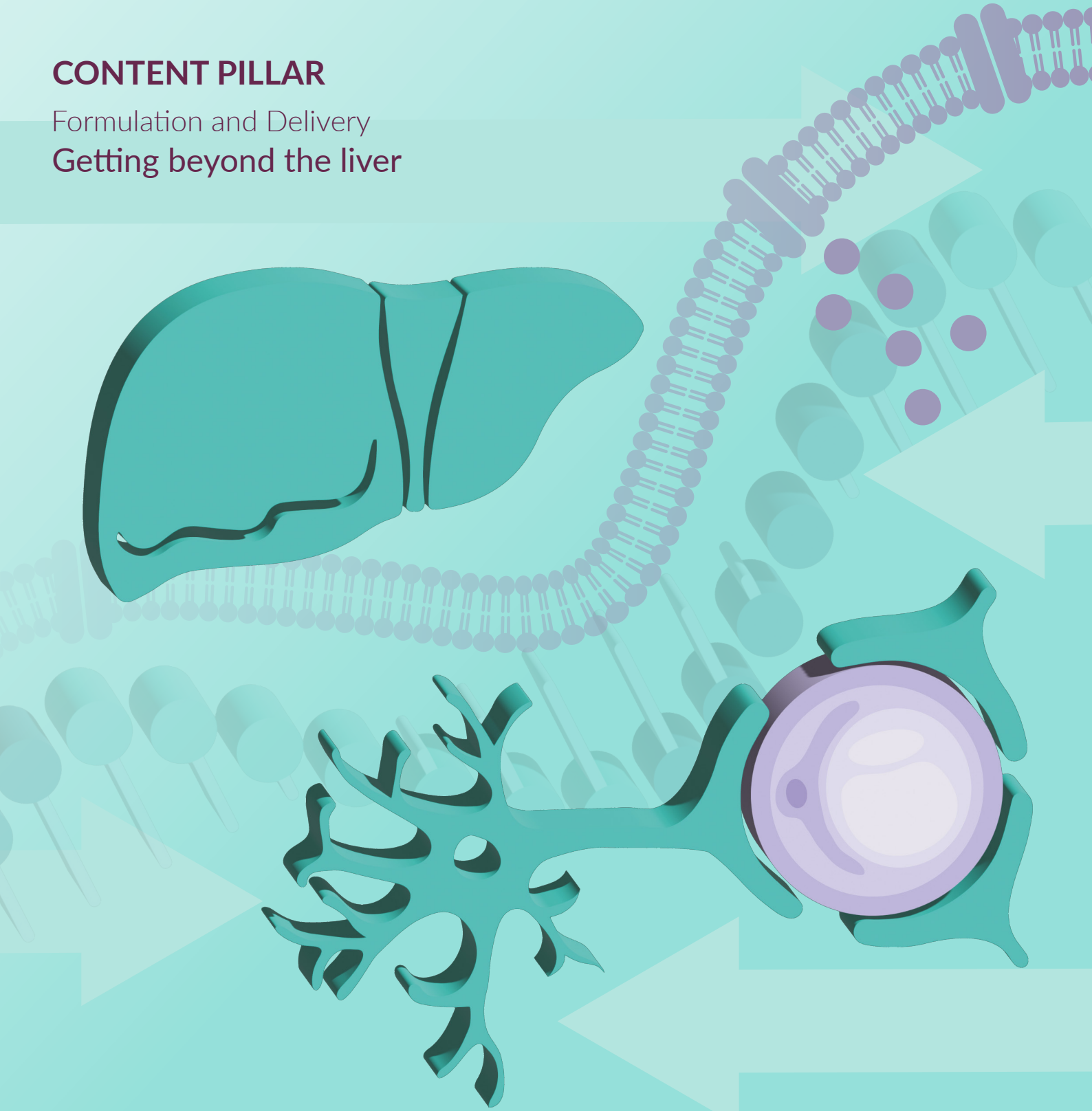

NUCLEIC ACID INSIGHTS

CONTENTS VOLUME 2 · ISSUE 6

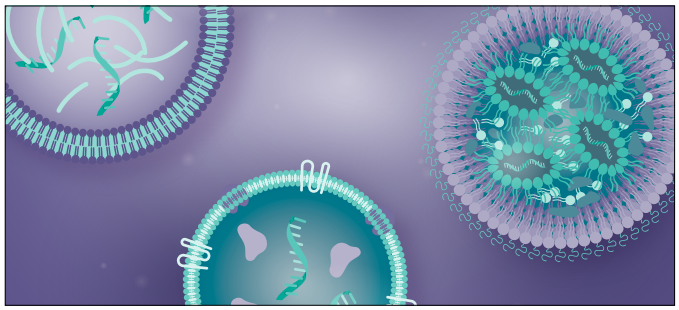

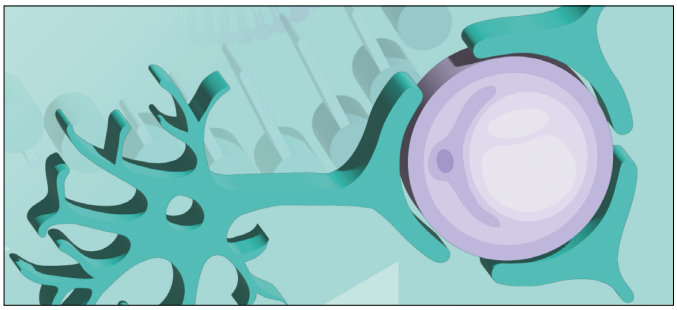

FORMULATION AND DELIVERY
Getting beyond the liver

LATEST ARTICLES

NUCLEIC ACID INSIGHTS

FORMULATION AND DELIVERY
GETTING BEYOND THE LIVER

SPOTLIGHT

EXPERT INSIGHT

Multifunctional pH-sensitive ionizable lipids for efficient nucleic acid delivery

Victoria EA Laney and Zheng-Rong Lu

Efficient nucleic acid delivery remains a critical challenge in gene therapy. This expert insight review discusses the design rationale of multifunctional pH-sensitive ionizable lipids, their structure-function relationships, and pH-sensitive amphiphilic endosomal escape and cytosolic cargo release, and examines a lead lipid ECO for nucleic acid therapeutics. ECO features an ethylenediamine headgroup (E), cysteine-based disulfide linkers (C), and distal oleoyl tails (O) that enable nucleic acid condensation through electrostatic and hydrophobic interactions. ECO spontaneously self-assemble with nucleic acids to form stable lipid nanoparticles (ELNP) without helper lipids or large volumes of organic solvent. Its pH-sensitive ionization facilitates site-specific endosomal escape, while redox-cleavable disulfide bonds in ELNP ensure cytosolic cargo release. We present case studies demonstrating ELNP's efficacy across diverse nucleic acid cargoes and provide comparative analysis against existing delivery systems. This work highlights the potential of multifunctional pH-sensitive ionizable lipids to overcome key barriers in nucleic acid delivery and outlines directions for clinical translation.

Nucleic Acid Insights 2025; 2(6), 131–148 · DOI: 10.18609/nuc.2025.019

INTRODUCTION

Nucleic acid therapeutics represent a promising class of gene therapy that treat diseases through various mechanisms, including gene silencing, protein expression, and gene manipulation. Since the COVID-19 pandemic of 2020, lipid-based nanoparticles (LNPs) have undergone a renaissance, particularly with increasing focus on their use for delivering nucleic acid therapeutics [1–4]. The clinical success of ionizable lipids in mRNA vaccines has validated this delivery approach and accelerated development of ionizable lipid systems for a diverse array of therapeutic nucleic acid applications [5,6]. Nucleic acid therapeutics include antisense oligonucleotides (ASOs), small interfering RNAs (siRNAs), microRNAs, messenger RNAs

(mRNAs), gene editors, and various forms of therapeutic DNA.

Despite numerous advances in nucleic acid therapeutics, their clinical translation has been hindered by several challenges, including poor stability in serum, limited cellular uptake, inefficient endosomal escape, potential immunogenicity, and rapid clearance from circulation [7,8]. Various delivery systems, including nonviral and viral systems, have been explored to address the challenges [3]. Viral systems, including adeno-associated virus (AAV) and lentiviral vectors, are highly efficient for gene delivery but often suffer from significant immunogenicity, manufacturing complexity, and high production costs that can exceed US$100,000 per dose [9]. To overcome these barriers and prevent unintended side effects, well-designed nanoparticle-based delivery platforms offer a relatively simple and cost-effective solution.

A wide array of lipid- and polymer-based nanoparticle systems has been developed for nucleic acid delivery, encompassing conventional cationic lipids, ionizable lipids, block copolymers, and hybrid constructs. While conventional cationic lipids or polymers are versatile for delivering various nucleic acids without size limitations, they are either toxic or inefficient for *in vivo* delivery. Cationic polymers, especially PEI based delivery systems, have been extensively investigated in preclinical studies, but have not reached broad clinical development due to concerns related to the safety and delivery efficiency for *in vivo* use [10,11]. Early cationic lipid systems, such as DOTMA (N-[1-(2,3-dioleyloxy) propyl]-N,N,N-trimethylammonium chloride) and DOTAP (1,2-dioleoyl-3-trimethylammonium-propane), demonstrated proof-of-concept for lipid-mediated gene delivery, but were limited by high toxicity and poor *in vivo* performance [12,13]. pH-sensitive ionizable lipids have been developed to address the limitations of cationic lipids. The ionizable lipids are neutral and non-amphiphilic at physiological pH during the delivery process and are protonated and become amphiphilic to facilitate for cytosolic cargo delivery [3,14,15].

Currently, ionizable lipid nanoparticles (LNPs) have become clinically dominant, exemplified by MC3, ALC-0315, or SM-102-based formulations in approved siRNA therapeutics or mRNA vaccines [16–21]. However, these ionizable lipids require helper lipids, a large volume of organic solvents, and complex formulation processes to form stable nanoparticles. These systems rely on a carefully optimized combination of ionizable lipids (30–50 mol%), helper lipids such as DSPC (1,2-distearoyl-sn-glycero-3-phosphocholine; 10–20 mol%), cholesterol (30–40 mol%), and PEG-lipids (1–3 mol%) to achieve LNP formulation, nucleic acid protection, optimal biodistribution, and intracellular delivery [21–23]. These multi-component systems require complex manufacturing processes including high-energy mixing, ethanol injection methods, extensive purification steps to remove organic solvents (typically >90% ethanol initially) through tangential flow filtration or dialysis [24–26].

Multifunctional pH-sensitive ionizable lipids represent constitute an engineered class of delivery materials designed to exploit to the pH gradients in subcellular trafficking and redox environments. Their tunable charge and structural features enable nucleic acid complexation, safe *in vivo* delivery, endosomal escape, and cytosolic cargo release. They are particularly promising candidates for local and systemic efficient delivery of therapeutic nucleic acids of any forms and sizes, including siRNA, miRNA, ASO, mRNA, plasmid DNA, and gene editors without using helper lipids. This capability depends on specific structural features including optimal lipid tail spacing, non-lamellar phase behavior, and precisely tuned combination of amino head groups and lipid tails. The multifunctionality of this class of ionizable lipids enables:

- The efficient incorporation of almost any nucleic acid payloads without helper lipids;
- Facile functionalization with targeting ligands to improve delivery specificity;
- Targeted delivery and cellular uptake via systemic delivery;
- Efficient amphiphilic endosomal escape in response to the pH decrease during subcellular trafficking; and
- Cytosolic cargo release [14,15,27–30].

A multifunctional ionizable lipid ECO ([1-aminoethyl]iminobis[N-(oleoylcysteinyl-1-amino-ethyl)propionamide]) and ECO-based lipid nanoparticles (ELNP) are identified as a lead versatile lipid platform for the delivery of a variety of nucleic acids [27].

This review discusses the design principles, functional mechanisms, properties, and applications of multifunctional pH-sensitive ionizable lipids for nucleic acid delivery, with particular emphasis on the lipid carrier, ECO. We examine the structure-function relationships of these ionizable lipids, their non-lamellar phase behaviors, and their endosomal escape mechanism that enable efficient cytosolic delivery of nucleic acid cargoes. Additionally, we discuss their potential for advancing the clinical development of nucleic acid-based therapeutics and provide comparative analysis with established delivery systems to contextualize ECO's advantages and limitations.

DESIGN PRINCIPLES OF MULTIFUNCTIONAL IONIZABLE LIPID CARRIERS

Endosomal escape remains a key step for cytosolic gene delivery. Conventional lamellar cationic lipids or ionizable lipids form stable lipid bilayers with helper lipids, which improve serum compatibility, reduce premature leakage or aggregation, and ultimately enhance *in vivo* performance. However, endosomal escape of the lamellar LNPs relies on lamellar-to-hexagonal phase transition, which is inefficient to mediate endosomal escape with only 1–2% of internalized cargo reaching the cytosol [31].

To address the limitation of conventional lamellar lipid systems, multifunctional pH-sensitive amphiphilic lipids have been explored by incorporating pH-sensitive amphiphilicity and environmentally responsive nucleic acid release mechanisms [14,28,32,33]. The multifunctional pH-sensitive amphiphilic lipids feature a pronounced wedge structure by integrating distal lipid tails, thereby preventing the formation of stable bilayers. These lipids are also known as non-lamellar amino lipids and can self-assemble with nucleic acids to form inverted hexagonal complexes. These amino lipids and their corresponding LNPs are designed to maintain relatively neutral charge states and to exhibit minimal amphiphilicity at physiological pH (7.4), ensuring safe systemic circulation. This mechanism is termed pH-sensitive amphiphilic endosomal escape, referring to the selective acquisition of membrane-disruptive amphiphilic properties specifically within the acidic endosomal environment (pH 5.5–6.5). The amino lipids undergo protonation specifically within the endosomal pH range (5.5–6.5), triggering the acquisition of amphiphilicity and membrane disruption. The electrostatic and amphiphilic interactions between these protonated non-lamellar lipids and endosomal membranes are meticulously calibrated to facilitate lipid membrane fusion and to induce membrane destabilization with the selectivity for the acidic compartments, ultimately facilitating efficient endosomal escape of the therapeutic cargo [14,15]. This mechanism is termed pH-sensitive amphiphilic endosomal escape. These pH-sensitive lipids

remain relatively inert at physiological pH but become potent membrane disruptors only when protonated in acidic ensodomes, ensuring selective endosomal targeting while minimizing off-target membrane damage.

Several critical structural and physicochemical considerations are incorporated in the design to avoid lipid bilayer formulation, to form stable LNP by self-assembly with nucleic acids, to facilitate safe and efficient cytosolic cargo delivery by sensing and responding to environmental changes during the delivery process. During systemic circulation, these lipid nanoparticles (LNPs) maintain relatively neutral, only becoming protonated in acidic endosomes to facilitate safe and efficient *in vivo* cytosolic delivery [15].

Structural design

Multifunctional pH-sensitive ionizable lipids typically comprise three essential domains: an amino head group, a linker, and a hydrophobic region with distal lipid tails. Each component plays a critical role in LNP formations and overcoming specific delivery barriers. Critically, unlike other reported ionizable amino lipids, multifunctional pH-sensitive amino lipids have two polymerizable thiol groups, which can be crosslinked by forming disulfide bonds via auto-oxidation to stabilize the lipid nanoparticles [14,27,33–35]. Some of the thiol groups can be used for facile modification with targeting agents and biocompatible polymers of the LNPs for systemic and targeted delivery [29,30,36–40].

- Amino/ionizable head groups: these groups are responsible for electrostatic interactions with negatively charged nucleic acids and provide pH-responsive behavior. Unlike permanently charged cationic head groups, ionizable head groups change their protonation state to become hydrophilic in response to environmental pH, enabling selective cellular and subcellular membrane interactions;

- Hydrophobic domains: the sections contain lipid tails that provide the lipophilic character necessary for nanoparticle condensation and membrane fusion. The composition, length, and degree of saturation of these domains significantly impact the fusion properties and phase transition behavior of the lipids. Two lipid tails are distant from each other to prevent forming lipid bilayers;

- Linkers: these chemical structures connect the head and tail domains and are used to adjust the distance between the lipid tails by varying their sizes. Functional groups such as polymerizable thiols are also incorporated in these regions to stabilize LNP and modification of LNP surface. No other helper lipids are needed for the multifunctional LNP stabilization and surface modification.

Rational design approach

Engineering pH-responsive ionizable lipids involves the deliberate selection and integration of amino head groups and lipid tails to achieve finely tuned protonation profiles that trigger intracellular membrane disruption specifically within the acidic endosomal environment. This critical head group-tail combination governs pH-sensitive amphiphilicity, which can be finely modulated through the incorporation of primary, secondary, and tertiary amines, imidazole moieties, and optimization of ionizable amino group density within the head structure. Here we outline the structure-activity relationships of each component. Head group architectures containing two or fewer ionizable amino groups, coupled with unsaturated lipid tails, have demonstrated

superior performance in mediating precisely controlled pH-triggered amphiphilic transitions required for efficient and site-specific endosomal escape. Extended molecular linkers spanning 13 atoms or more between lipid tails effectively disrupt bilayer stabilization, promoting non-lamellar phase behavior essential for membrane fusion and destabilization [14,27,33–35]. Incorporation of cysteine residues enables disulfide cross-linking (improving stability) and provides attachment points for targeting ligands.

Key physicochemical characteristics

The delivery efficiency of the multifunctional lipids is significantly influenced by their physicochemical properties, including pK_a, ionization, molecular assembly, and pH-sensitive membrane disruption. The pK_a of the ionizable head group is critical for pH-responsive behavior and represents a key distinction from conventional cationic lipids. Ideally, the lipid should be minimally charged at physiological pH (7.4) to reduce toxicity and non-specific interactions, but become increasingly protonated as pH decreases in endosome (pH 5. to −6.5). The pK_a of the protonatable amines in the head groups ranges from 7.6–10.7 and ~6.0 for imidazole group in histidine. However, it is the combination of the number of the protonatable amino groups in the head groups and lipids that determines controlled pH-sensitive membrane disruption at the endosomal pH [27,28,33–35,41]. pH-dependent ionizability is also crucial for safe systemic nucleic acid delivery as it minimizes hemotoxicity and cytotoxicity at physiological pH, enhanced endosomal escape in acidic environments.

A critical distinction from other lipids is the non-lamellar feature of the multifunctional ionizable lipids that facilitate efficient endosomal escape [15,28]. Lamellar lipids (lipids that form bilayer structures similar to cell membranes), including lamellar ionizable lipids, rely on the lamellar to inverted hexagonal phase transition mechanism for endosomal escape [42–45]. This process requires significant energy input and coordination between multiple lipid molecules, making it inherently inefficient, typical endosomal escape rates for lamellar systems in the range of 1–5% of internalized particles [31,46]. In contrast, multifunctional ionizable lipids do not form stable lipid bilayers due to their wedge-shaped molecular geometry and extended linker regions. This architectural design bypasses the lamellar to inverted hexagonal phase transition, instead facilitating direct membrane disruption via protonated lipid membrane fusion of a micellar intermediate in acidic endosomes. This mechanism enables highly efficient endosomal escape (up to 80% of internalized particles) and correspondingly greater transfection efficiency compared to conventional lamellar ionizable lipids.

ECO BASED LIPID NANOPARTICLES (ELNP)

Structural features of ECO

ECO represents a promising versatile delivery platform for cytosolic delivery of a variety of therapeutic nucleic acids, **Figure 1** [30,37,47,48]. It consists of three key structural components, an ethylenediamine (E) head group with containing primary and tertiary amines, a linker with two cysteinyl residues (C), and two distal mono-unsaturated oleoyl (O) tails. ECO has a wedge-shaped molecular geometry of a large lipophilic area, which prevents forming stable lipid bilayer and contributes to pH-sensitive membrane interaction, fusion, and disruption.

Formulation of ELNP with various nucleic acids

Due to its multifunctionality, ECO forms stable ELNPs with nucleic acids of any

FIGURE 1

Formulation of targeted ELNP.

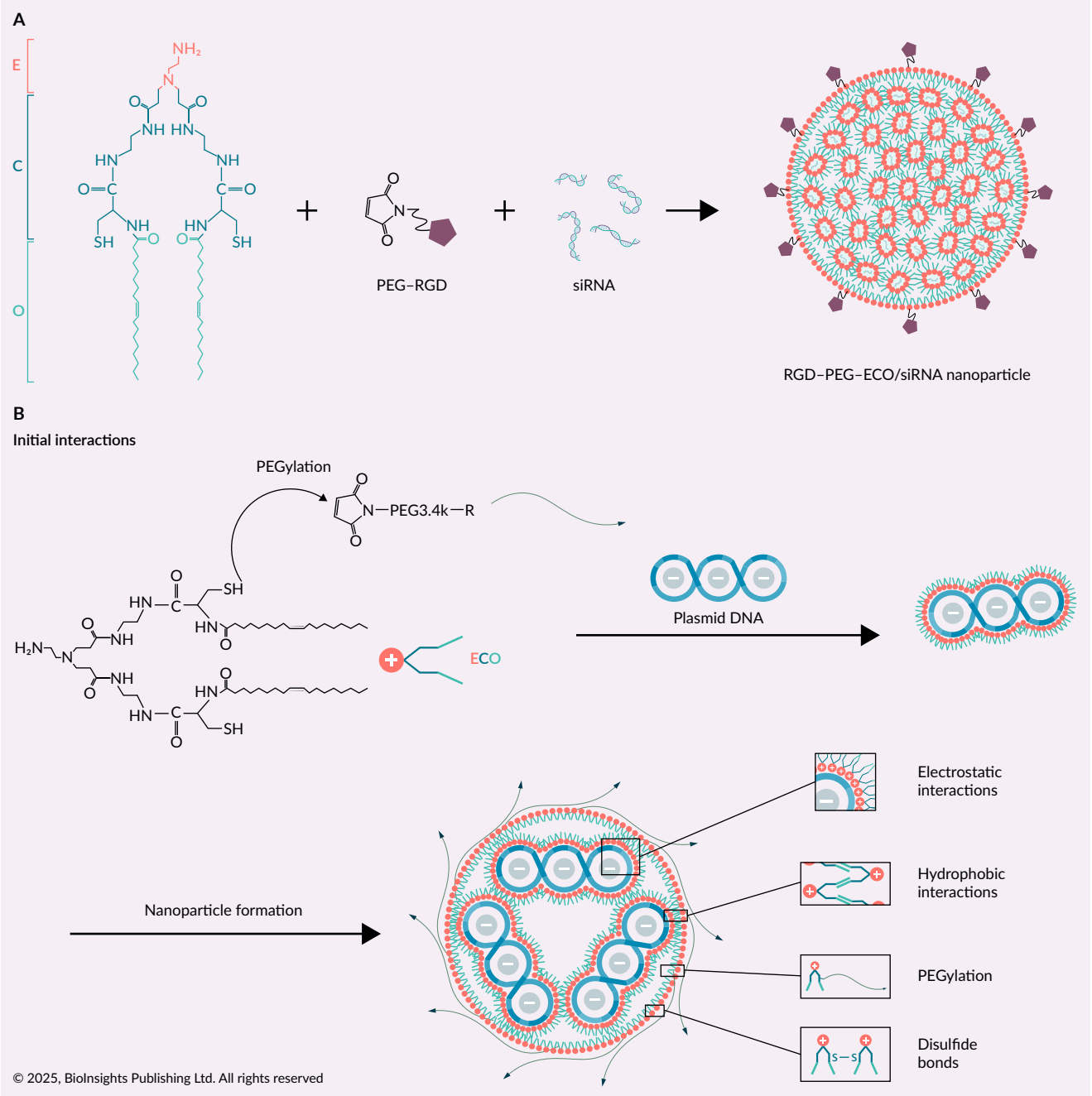

(A) Formation of functionalized and targeted ECO lipid nanoparticles (ELNP) with siRNA. ECO encapsulates siRNA and to form targeted ELNP, RGD-PEG-ELNP/siRNA, by attaching a targeting motif via a PEG spacer to small portion of the thiols on ECO (~2.5 mol-%).
(B) Similarly, ELNP of large plasmid DNA can be functionalized with targeting ligands for enhanced delivery [48,51]. R: functional targeting ligand. © 2025, BioInsights Publishing Ltd. All rights reserved.

forms and sizes without any helper lipids to protect the cargo during systemic circulation and endocytic trafficking. It self-assembles with DNA, RNA, or gene editors to form stable nanoparticles through a combination of electrostatic complexation, hydrophobic condensation of the lipid tails, and disulfide bond cross-linking

of the cysteinyl residues via autoxidation. No helper lipids are needed for ELNP formulation. Notably, only a very small amount of organic solvent (~5% ethanol of total final volume) is needed during the formulation process. The standard formulation of ELNP uses a low ethanol content (5%, v/v), which facilitates rapid nano-formulation of lipid-nucleic acid complexes while minimizing post-formulation purification. Ethanol has been commonly used as solvents in pharmaceutical formulations [49,50]. While the small amount of ethanol does not affect the ELNP stability and no extra steps are needed to remove ethanol. Nevertheless, future studies could further investigate the potential clinical impact of residual ethanol levels in accordance with ICH Q3C guidelines followed by the European Medicines Agency (EMA) and the US FDA. Targeting agents can be readily incorporated onto the LNP surface by reacting with a small portion of the thiol groups (~2.5 molar-% of ECO). **Figure 1** illustrates the examples of formation of stable targeted ELNPs with siRNA and large plasmid DNA. The sizes of ELNP are consistently in the range of 80–150 nm [28].

The ratio of protonatable amino groups of the lipids to phosphates in nucleic acids, also known as N/P ratio, plays a critical role for encapsulation of nucleic acids. Low N/P ratios (less than 4) consistently result in incomplete complexation and produce larger particles with reduced stability. The optimal N/P ratios for ELNPs range from 6 to 12. High N/P ratios (greater than 15) often result in increased cytotoxicity. Nucleic acid size also affects ELNP encapsulation efficiency. ECO demonstrates excellent siRNA encapsulation, achieving over 90% efficiency at N/P ratios above 8 [27]. Complete plasmid DNA encapsulation can be achieved at an N/P ratio of 6 [35]. ELNPs with an N/P ratio of 8 have demonstrated excellent safety and delivery efficiency with repeated systemic and local injections in preclinical experiments [30,51].

pH-sensitive amphiphilic membrane disruption and endosomal escape of ELNP

A defining characteristic of ECO is its well-controlled pH-sensitive cell membrane disruption, which is essential for efficient site-specific endosomal escape. The ethylenediamine head group of ECO in ELNPs has minimal protonation at physiological pH (7.4) and increasingly charged as pH decreases in early endosomes (pH = 6.5) and later endosomes (pH = 5.5), resulting in selective membrane-disruptive properties, **Figure 2A** [15,27].

The cellular uptake of ELNP/siRNA involves multiple endocytic mechanisms, including receptor-mediated endocytosis, clathrin-mediated endocytosis, caveolae-mediated endocytosis, and macropinocytosis. After internalization, nanoparticles follow the endosomal-lysosomal pathway, progressing from early endosomes (pH ~6.5) to late endosomes (pH ~5.5) [15]. As shown in **Figure 2B**, significant dispersion of red fluorescence labeled siRNA is observed in the cytoplasm at 4 hour after incubation, indicating endosomal escape and cytosolic release of the cargo.

Beyond pH-sensitive membrane disruption, ELNP incorporates an additional mechanism for controlled intracellular release through its cysteine residues. During nanoparticle formation, the thiol groups can undergo autooxidation to form intermolecular disulfide bonds, stabilizing the ELNP and preventing premature siRNA release. Upon entering the cytosol, these bonds encounter the reducing environment created by high intracellular glutathione (GSH) concentrations (1–15 mM vs 1–10 μM extracellular), leading to bond cleavage, nanoparticle disassociation, and cargo release [15]. This pH-sensitive amphiphilic endosomal escape and

FIGURE 2

ELNPs mediate efficient pH-sensitive amphiphilic endosomal escape and cytosolic nucleic acid delivery.

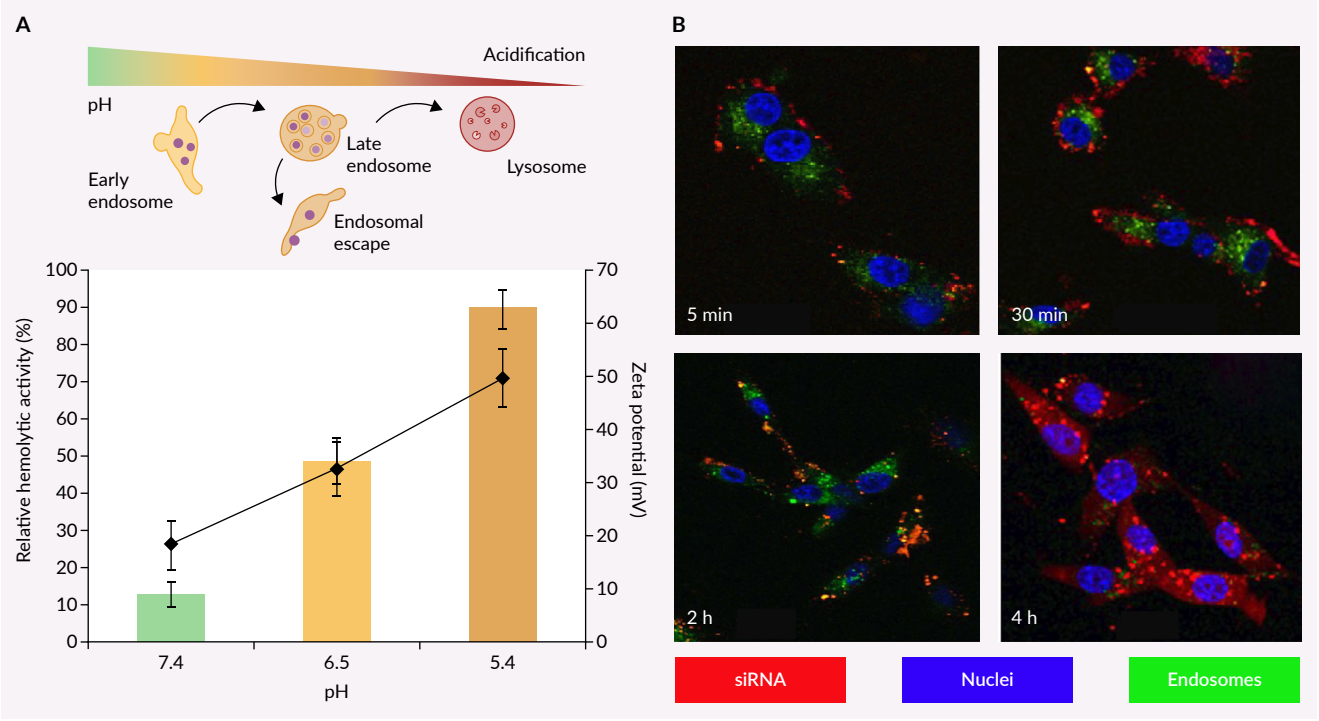

(A) Schematic of pH-sensitive endosomal escape mechanism of ELNP/siRNA and increase of surface charges and cell membrane disruption shown as hemolysis from neutral pH, early endosomal pH, and late endosomal pH due to increasing protonation and amphiphilicity.
(B) Confocal immunofluorescence imaging of particle internalization into endosomes and siRNA release in cytoplasm [15].

reductive cytosolic release (PERC effect) provides precise spatiotemporal control over cytosolic cargo delivery, ensuring that the payload remains protected until it reaches the cytosolic environment [47].

APPLICATIONS IN NUCLEIC ACID DELIVERY

ELNP for targeted delivery of siRNA and miRNA in cancer therapy

ELNPs can be readily modified with targeting agents for systemic, targeted delivery of siRNA and miRNA, enabling efficacious cancer therapy. ELNP/siRNA systems have demonstrated remarkable efficiency in siRNA delivery and gene silencing, showing potent and sustained *in vitro* gene silencing with over 80% knockdown in certain cell types for at least 7 days. In mouse models, repeated systemic delivery of siRNA targeting overexpressed β3 integrin (siβ3) significantly inhibited the proliferation of triple-negative breast cancer (TNBC) [30]. ELNP/siβ3 treatment also prevented the development of lung metastases in preclinical TNBC, **Figure 3A**. Targeted delivery of siRNA against a gene target eIF4E with targeted ELNP also sensitized drug resistant cancer cells to a chemotherapeutic agent, resulting in regression of drug resistance TNBC [47].

Long non-coding RNAs (lncRNAs) have emerged as crucial players in all aspects of oncogenic signaling. LncRNAs are long (>200 nucleotide) non-protein coding, endogenously transcribed RNA transcripts. Initially thought to be fragments of 'junk DNA', lncRNAs have now been established as functionally versatile species that exert multilevel gene regulation [52,53].

FIGURE 3

Targeted ELNPs facilitate effective tumor siRNA or miRNA delivery and anticancer treatment via systemic delivery.

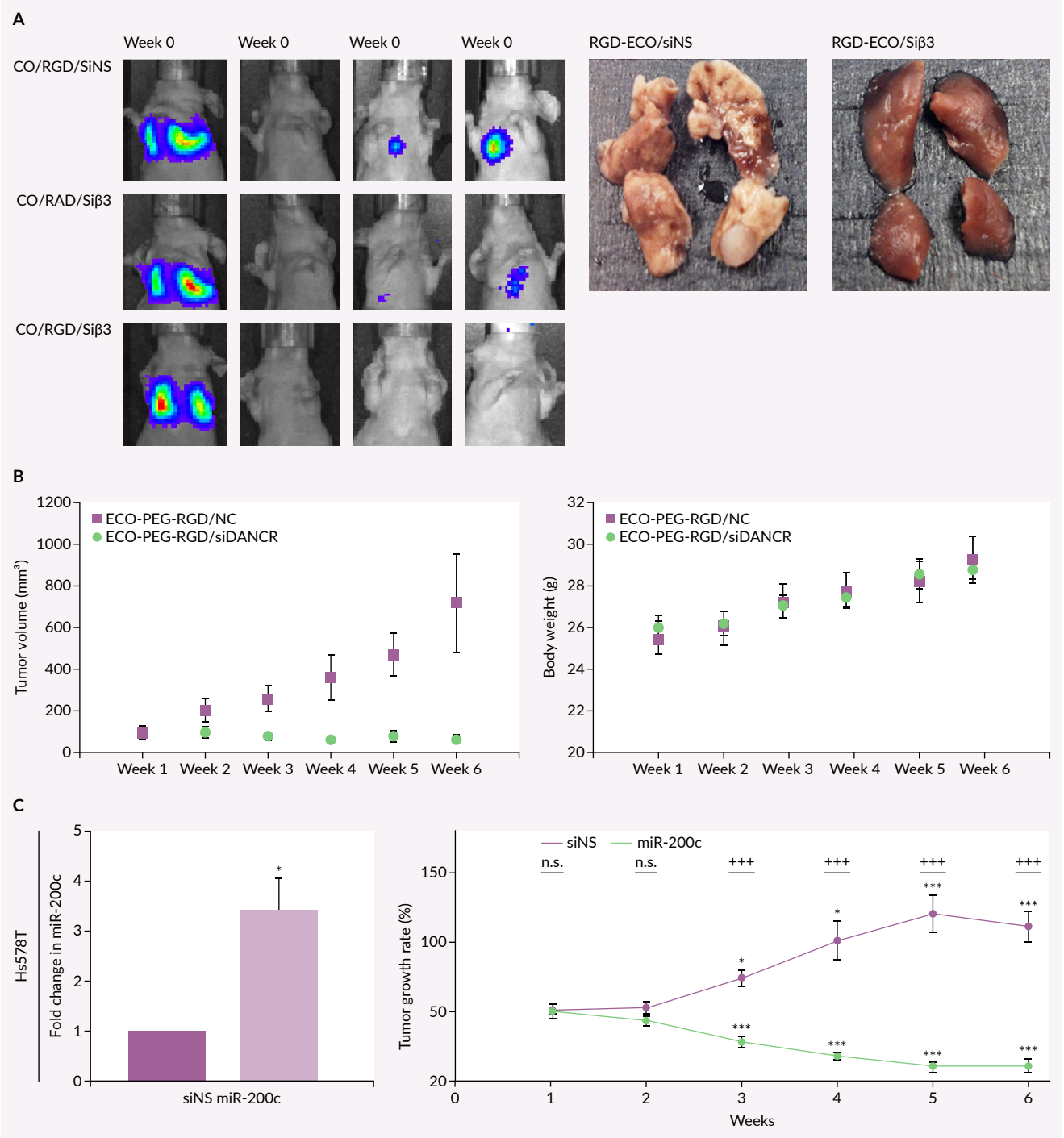

(A) Systemic administration of RGD peptide targeted ELNP/sib3 every 5 days at a dose of 1.5 mg-siRNA/kg inhibited lung metastasis of breast cancer in mice. (B) Systemic administration of RGD-PEG-ELNP/siDANCR weekly at a dose of 1.0 mg-siRNA/kg significantly inhibited tumor growth with little toxic side effects. (C) Systemic administration of RGD-PEG-ELNP/miR-200c weekly at a dose of 1.0 mg-miRNA/kg significantly restored the miR-200c level in the tumors, resulting in tumor regression [30,38,39].

Repeated systemic administration of ELNP/siDANCR resulted in significant silencing of an oncogenic lncRNA DANCR, allowing for modulation of cancer pathways and suppression of tumor growth, **Figure 3B [39]**. Additionally, targeted ELNP/siDANCR treatment showed potential to alleviate drug resistance in TNBC **[40]**.

MicroRNA (miRNA) plays an essential role in regulating cancer pathways and represents a promising class of cancer therapeutics **[54,55]**. The miR-200 family, including miR-200a, miR-200b, miR-200c, miR-141, and miR-429, acts as 'guardians of the epithelial phenotype' by suppressing the epithelial-mesenchymal transition (EMT) **[56]**. Among these, miR-200c has been identified as a key tumor suppressor that regulates EMT in aggressive tumors. Systemic administration of targeted ELNP/miR-200c restored miR-200c levels in tumors and downregulated oncoproteins associated with EMT, resulting in inhibition and regression of triple-negative breast cancer (TNBC) in mice, as shown in **Figure 3B [38]**. In pancreatic ductal adenocarcinoma (PDAC) models, treatment with RGD-ELNP/miR-200c demonstrated significant tumor extracellular matrix remodeling and reduced fibronectin expression, consistent with decreased mRNA levels in extracted tumors **[57]**.

ELNP for efficient delivery of plasmid DNA in gene therapy

ELNP is a promising delivery platform for therapeutic DNA for gene therapy. ECO readily forms stable ELNP with therapy plasmid DNA via self-assembly for gene therapy with an excellent safety profile **[37,51,58–61]**. ELNP/*pCMV-GFP* exhibited comparable or higher *in vitro* gene transfection efficiency than AAV2-*CMV-GFP* in ARPE-19 cells **Figure 4A [51]**. An ACU-4429 (emixustat, EM or ACU) targeted ELNP, ACU-PEG-HZ-ELNP/*pCMV-GFP* resulted in robust expression of GFP in broader areas of the retina of *BALB/c* mice as compared to AAV after single subretinal injection at the same DNA dose with minimal inflammatory reaction, while significant tissue damage by inflammation was observed for the AAV-treated eyes, persistent for at least 3 months **Figure 4B [51]**.

ELNPs of the plasmid DNA expressing RPR65 or ABCA4 have been tested for gene therapy of retinal disorders in mouse models. Single subretinal injection of an all-trans-retinylamine-modified ELNP/*pRPE65* in Rpe65$^{-/-}$ mice, a mouse model of Leber's congenital amaurosis type 2 (LCA2), significant increased electroretinographic activity and cone photoreceptor preservation lasting at least 120 days **[37]**. Because of the low immunogenicity, repeated subretinal injections of PEGylated ELNPs carrying a large plasmid *pGRK1-ABCA4-S/MAR* (11.6 kb) (PEG-ELNP/*pGRK1-ABCA4-S/MAR,* 150 nm) resulted in increased and prolonged ABCA4 expression for >11 months throughout the retina in *abca4*$^{-/-}$ mice, a mouse model of Stargardt disease, **Figure 4C [51]**. The use of repeated subretinal injections did not affect the visual function of the mice as shown by both scotopic and photopic electroretinography (ERG). Repeated intravitreous injections of two doses of PEG-ELNP/*pGRK1-ABCA4-S/MAR* also resulted in significant expression of ABCA4 in the photoreceptor cells, **Figure 4D [62]**.

ELNP for delivery of gene editors in gene editing

ECO forms stable ELNPs with a plasmid-DNA expressing sgRNA (*psgRNA*) (9.4 kb) and a plasmid DNA expressing Cas9 (*pCas9*; 13.6 kb), respectively, through self-assembly and simple agitation at N/P ratios of 6, 8 and 10. The ELNPs had a narrow size distribution between 120 and 150 nm at the tested N/P ratios. The ELNP exhibited no cytotoxicity to NIH3T3-GFP cells. The ELNP demonstrated precisely

FIGURE 4

Pegylated ELNPs facilitate efficient delivery of therapeutic plasmid DNA delivery to treat retinal degenerations.

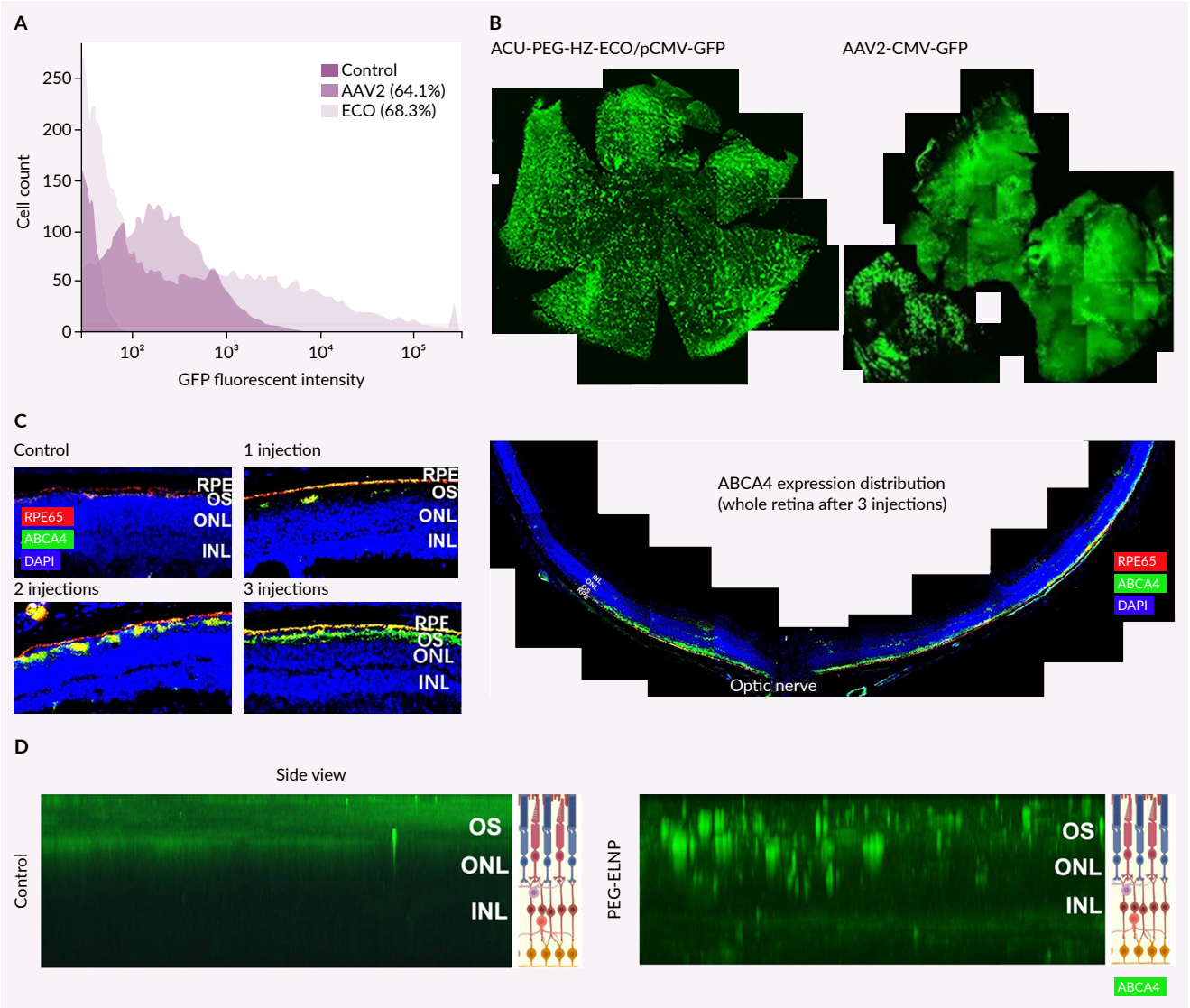

(A) Flow cytometry of GFP expression in ARPE-19 cells, 48 hours after transfection with ECO/pCMV-GFP or AAV-CMV-GFP. (B) Fluorescence-microscopic images of GFP expression (green dots) in the retinal flatmounts of mice treated with ACU-PEG-HZ-ECO/pCMV-GFP or AAV2-CMV-GFP 2 months after injection. Immunofluorescence staining of ABCA4 in photoreceptors of Abca4$^{-/-}$ mice after (C) subretinal injections and (D) two intravitreal injections of PEG-ECO/pGRK1-ABCA4-S/MAR [51,62]. ELNP, RGD-PEG-ELNP/siRNA, by attaching a targeting motif via a PEG spacer to small portion of the thiols on ECO (~2.5 mol-%). (B) Similarly, ELNP of large plasmid DNA can be functionalized with targeting ligands for enhanced delivery [48,51].

controlled pH-sensitive cell membrane disruption with the background activities at pH 7.4, ~45% of hemolytic activity at pH 6.5 (early endosomal pH), and ~95% hemolysis at pH 5.5 (late endosomal pH) [35].

The ELNP mixture of CRISPR/Cas9 plasmids mediated substantial transfection of Cas9 and sgRNA in NIH3T3-GFP cells. Confocal fluorescence imaging also revealed significant GFP knockdown when compared to untreated cells and cells treated with LNP of commercial lipofectamine-2000 **Figure 5A**. GFP knockdown efficiency (~80%) was also confirmed at mRNA level by qRT-PCR **(Figure 5B)**. Significant expression of Cas9 protein in

FIGURE 5

ELNPs mediate effective gene editing with CRISPR/Cas9.

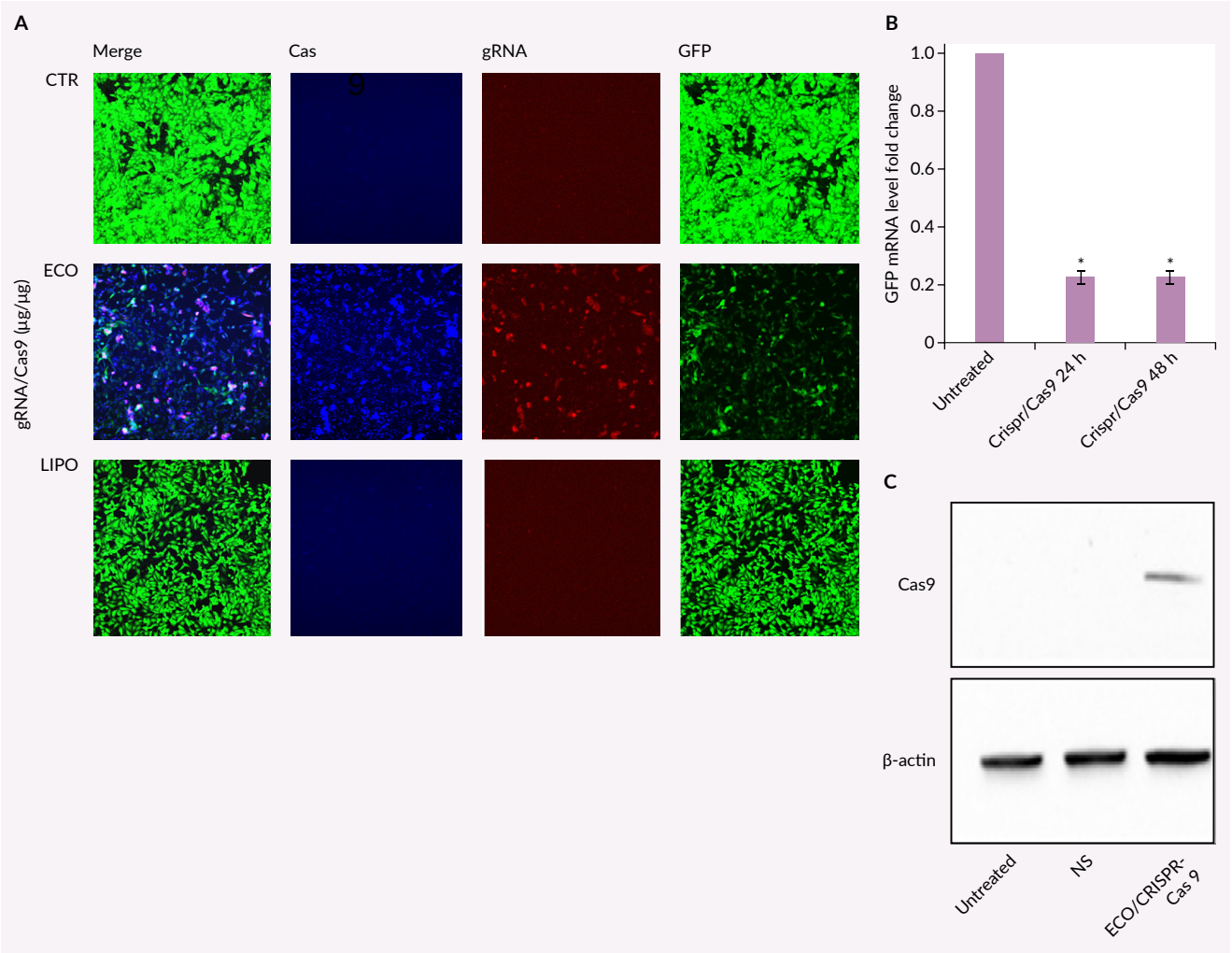

(A) ECO mediates higher expression of Cas9 (blue) and sgRNA (red), and GFP knockdown than lipofectamine-2000 in NIH3T3-GFP cells at the dose of each plasmid at 1.5 μg/well in 12 well plates. (B) GFP knockdown efficiency at mRNA levels. (C) Western blot showing Cas9 protein expression after 72h.*p<0.05 **[35]**. ELNP, RGD-PEG-ELNP/siRNA, by attaching a targeting motif via a PEG spacer to small portion of the thiols on ECO (~2.5 mol-%). (B) Similarly, ELNP of large plasmid DNA can be functionalized with targeting ligands for enhanced delivery **[48,51]**.

the transfected cells was also determined by Western blotting **(Figure 5C) [35]**.

COMPARATIVE ADVANTAGES OF ELNP

As compared to other ionizable lipids, ELNPs are formulated without helper lipids, while other lipids such as MC3, ALC-0315, and SM-102 rely on helper lipids to form stable particles. The other reported ionizable lipids often have excellent lipophilicity and poor water solubility, and require a high volume of ethanol in LNP formulation. Extra steps of dialysis and purification are needed to remove excess ethanol. In contrast, ECO has a large hydrophilic head group and better water solubility, and needs only 5% of ethanol of the total solvent volume in the formulation. The formulation step of ELNP is straightforward and no extra step is needed for purification, thereby streamlining production procedures.

The ELNP platform demonstrates exceptional capacity and versatility for safe, efficient delivery of diverse therapeutic nucleic acids for cancer therapy, gene therapy, and gene editing. Its multifunctional design enables straightforward formulation of stable ELNPs with nucleic acids ranging from small siRNAs (21 nucleotides) to large plasmid DNA constructs (>10 kb), a significant advantage over most reported ionizable lipids, which are typically optimized for specific nucleic acid types and size ranges. ELNP has shown excellent delivery efficiency of nucleic acids in cancer therapy and gene therapy in a variety of preclinical models.

The platform's precisely calibrated pH-sensitive membrane disruption at endosomal pH substantially reduces cytotoxicity compared to permanently charged cationic lipids during both local and systemic delivery, while ELNP facilitates efficient endosomal escape and cytosolic cargo release through its dual pH-sensitive and redox-responsive mechanisms. Notably, unlike many competing technologies, ECO maintains its performance advantages even in challenging serum-containing conditions that closely mimic *in vivo* environments, where many delivery systems exhibit significantly compromised efficiency. The accessible thiol groups inherent to ECO's structure provide versatile attachment points for surface modifications, programing ELNP's functionality for specific applications and expanding possibilities for diverse therapeutic approaches.

CRITICAL LIMITATIONS & CHALLENGES

Despite these advantages, several challenges remain to be systematically addressed for clinical translation of ELNP. A significant limitation is the lack of human safety data compared to the clinically used ionizable LNPs. Comprehensive toxicology studies including repeated-dose studies, biodistribution analysis, and immunogenicity assessment are essential prerequisites for regulatory submission, along with establishing manufacturing processes that meet GMP standards for clinical production. There might be a concern that the disulfide linkages in ELNP could be prematurely reduced by glutathione in blood plasma during systemic delivery. However, the concentration of glutathione in normal plasma is in the range of 1–10 μM. Our unpublished study showed that the ELNPs were stable in the presence of such low glutathione concentrations and dissociated at the cytosolic concentration of glutathione (1–15 mM). Nevertheless, further work is needed to determine the influence of the environmental redox conditions on nanoparticle integrity and pharmacokinetics across diverse patient populations.

Given the potential for repeated administration in chronic disease settings, long-term biocompatibility and immunogenicity of ECO-based nanoparticles require comprehensive evaluation. To date, ELNP has not elicited overt immune activation in rodent studies, but comprehensive safety evaluations will be required prior to clinical translation. Chemistry, manufacturing, and controls (CMC) programs needs to be established for regulatory compliance.

TRANSLATIONAL OUTLOOK

Beyond the applications already discussed, a key future direction involves developing ELNP/mRNA formulations for vaccines targeting infectious diseases and cancer, as well as for gene editing applications where ECO's unique properties offer distinct advantages. ELNP demonstrates significant promise for mRNA delivery, particularly unmodified mRNA where conventional systems often struggle with stability and efficiency. Moreover, ELNP could be particularly effective for ribonucleoprotein delivery in gene editing applications due to the minimal organic solvent

required in formulation, which preserves protein stability and functionality that is often compromised in conventional LNP systems.

ECO's unique properties position it optimally for applications where conventional LNPs face significant limitations. The platform shows exceptional promise for large nucleic acid delivery, including plasmid DNA (>5 kb) and large mRNA constructs where ECO's size-independent formulation provides substantial advantages. Additionally, chronic diseases requiring repeated administration represent an attractive application where ELNP's reduced immunogenicity [48] can avoid the accelerated blood clearance phenomena that compromise long-term efficacy of traditional LNP systems.

ELNP-encapsulated ribonucleoproteins may offer substantial advantages over plasmid or mRNA-based gene editors, potentially yielding superior editing efficiency through fast editing kinetics and elimination of immunogenic DNA delivery concerns. The platform's simplified formulation process enables rapid prototyping of personalized mRNA therapeutics, particularly for cancer immunotherapy where patient-specific neoantigen vaccines require fast turnaround times between tumor sequencing and treatment initiation. Future research will also focus on optimizing the chemical structures of multifunctional pH-sensitive ionizable lipids to completely eliminate organic solvents in LNP formulation while enhancing lipid biodegradability.

SUMMARY

The development of multifunctional pH-sensitive ionizable lipids relies on the PERC effect (pH-sensitive amphiphilic endosomal escape and reductive cytosolic release) for effective nucleic acid delivery. Rational design and optimization of these lipid structures enables precise pH-sensitive membrane disruption, marking a substantial advancement in addressing fundamental challenges to cytosolic nucleic acid delivery. This breakthrough approach to precisely controlled membrane disruption and endosomal escape has since been widely adopted and helped in the design of various ionizable lipid systems for nucleic acid delivery.

While initial applications centered primarily on siRNA delivery for oncology applications, the platform's utility has expanded to include plasmid DNA, mRNA, and CRISPR-Cas9 delivery across different diseases. The platform's versatility across diverse nucleic acid cargoes demonstrates broader applicability than single-purpose delivery systems optimized for specific cargos. From a clinical translation perspective, while ECO remains in preclinical development, its unique advantages, simplified manufacturing, efficient endosomal escape, size-independent formulation, and reduced immunogenicity, position it to address unmet clinical needs. As the field advances toward personalized medicine and complex genetic interventions, ECO's modular design and rapid formulation capabilities may prove crucial for next-generation therapeutics requiring patient-specific customization or multi-component delivery.

By continuing to refine the molecular architecture of multifunctional pH-sensitive ionizable lipids while expanding their therapeutic applications, these delivery systems are well-positioned to overcome the persistent challenges that have limited the clinical translation of genetic medicines. The integration of simplified manufacturing, enhanced delivery efficiency, and reduced toxicity profiles represents a significant step toward realizing the full therapeutic potential of nucleic acid-based therapeutics across diverse clinical applications.

REFERENCES

1. Palanki R, Bose SK, Dave A, *et al.* Ionizable lipid nanoparticles for therapeutic base editing of congenital brain disease. *ACS Nano* 2023; 17(14),13594–13610.
2. Hald Albertsen C, Kulkarni JA, Witzigmann D, *et al.* The role of lipid components in lipid nanoparticles for vaccines and gene therapy. *Adv. Drug Deliv. Rev.* 2022; 188, 114416.
3. Sun D, Lu ZR. Structure and function of cationic and ionizable lipids for nucleic acid delivery. *Pharm. Res.* 2023; 40(1), 27–46.
4. Fenton OS, Kauffman KJ, McClellan RL, *et al.* Customizable lipid nanoparticle materials for the delivery of siRNAs and mRNAs. *Angew. Chem. Int. Ed. Engl.* 2018; 57(41), 13582–13586.
5. Polack FP, Thomas SJ, Kitchin N, *et al.* CCT Group, safety and efficacy of the BNT162b2 mRNA COVID-19 vaccine. *N. Engl. J. Med.* 2020; 383(27), 2603–2615.
6. El Sahly HM, Baden LR, Essink B, *et al.* Efficacy of the mRNA-1273 SARS-CoV-2 vaccine at completion of blinded phase. *N. Engl. J. Med.* 2021; 385(19), 1774–1785.
7. Tan X, Jia F, Wang P, *et al.* Nucleic acid-based drug delivery strategies. *J. Control. Release* 2020; 323, 240–252.
8. Gokirmak T, Nikan M, Wiechmann S, *et al.* Overcoming the challenges of tissue delivery for oligonucleotide therapeutics. *Trends Pharmacol. Sci.* 2021; 42(7), 588–604.
9. Collins LT, Ponnazhagan S, Curiel DT. Synthetic biology design as a paradigm shift toward manufacturing affordable adeno-associated virus gene therapies. *ACS Synth. Biol.* 2023; 12(1), 17–26.
10. Fattahi N, Gorgannezhad L, Masoule SF, *et al.* PEI-based functional materials: Fabrication techniques, properties, and biomedical applications. *Adv. Colloid Interface Sci.* 2024; 325, 103119.
11. Yang W, Mixich L, Boonstra E, *et al.* Polymer-based mRNA delivery strategies for advanced therapies. *Adv. Healthc. Mater.* 2023; 12(15), e2202688.
12. Liu F, Qi H, Huang L, *et al.* Factors controlling the efficiency of cationic lipid-mediated transfection *in vivo* via intravenous administration. *Gene Ther.* 1997; 4(6), 517–523.
13. Filion MC, Phillips NC. Toxicity and immunomodulatory activity of liposomal vectors formulated with cationic lipids toward immune effector cells. *Biochim. Biophys. Acta* 1997; 1329(2), 345–356.
14. Wang XL, Ramusovic S, Nguyen T, *et al.* Novel polymerizable surfactants with pH-sensitive amphiphilicity and cell membrane disruption for efficient siRNA delivery. *Bioconjug. Chem.* 2007; 18(6), 2169–2177.
15. Gujrati M, Malamas A, Shin T, *et al.* Multifunctional cationic lipid-based nanoparticles facilitate endosomal escape and reduction-triggered cytosolic siRNA release. *Mol. Pharm.* 2014; 11(8), 2734–2744.
16. Binici B, Rattray Z, Zinger A, *et al.* Exploring the impact of commonly used ionizable and pegylated lipids on mRNA-LNPs: a combined *in vitro* and preclinical perspective. *J. Control. Release* 2025; 377, 162–173.
17. Ferraresso F, Strilchuk AW, Juang LJ, *et al.* Comparison of DLin-MC3-DMA and ALC-0315 for siRNA delivery to hepatocytes and hepatic stellate cells. *Mol. Pharm*. 2022; 19(7), 2175–2182.
18. Paloncyova M, Cechova P, Srejber M, *et al.* Role of ionizable lipids in SARS-CoV-2 vaccines as revealed by molecular dynamics simulations: from membrane structure to interaction with mRNA fragments. *J. Phys. Chem. Lett.* 2021; 12(45), 11199–11205.
19. Basha G, Novobrantseva TI, Rosin N, *et al.* Influence of cationic lipid composition on gene silencing properties of lipid nanoparticle formulations of siRNA in antigen-presenting cells. *Mol. Ther.* 2011; 19(12), 2186–2200.
20. Kulkarni JA, Witzigmann D, Chen S, *et al.* Lipid nanoparticle technology for clinical translation of siRNA therapeutics. *Acc. Chem. Res.* 2019; 52(9), 2435–2444.
21. Sabnis S, Kumarasinghe ES, Salerno T, *et al.* A novel amino lipid series for mRNA delivery: improved endosomal escape and sustained pharmacology and safety in non-human primates. *Mol. Ther.* 2018; 26(6), 1509–1519.

22. Lokugamage MP, Vanover D, Beyersdorf J, *et al.* Optimization of lipid nanoparticles for the delivery of nebulized therapeutic mRNA to the lungs. *Nat. Biomed. Eng.* 2021; 5(9), 1059–1068.

23. Mui BL, Tam YK, Jayaraman M, *et al.* Influence of polyethylene glycol lipid desorption rates on pharmacokinetics and pharmacodynamics of siRNA lipid nanoparticles. *Mol. Ther. Nucleic Acids* 2013; 2(12), e139.

24. Belliveau NM, Huft J, Lin PJ, *et al.* Microfluidic synthesis of highly potent limit-size lipid nanoparticles for *in vivo* delivery of siRNA. *Mol. Ther. Nucleic Acids* 2012; 1(8), e37.

25. Gilbert J, Sebastiani F, Arteta MY, *et al.* Evolution of the structure of lipid nanoparticles for nucleic acid delivery: from *in situ* studies of formulation to colloidal stability. *J. Colloid Interface Sci.* 2024; 660, 66–76.

26. Driskill MM, Coates IA, Hurst PJ, *et al.* Lyophilized SARS-CoV-2 self-amplifying RNA vaccines for microneedle Array patch delivery. *J. Control. Release* 2025; 384, 113944.

27. Malamas AM, Gujrati M, Kummitha CM, *et al.* Design and evaluation of new pH-sensitive amphiphilic cationic lipids for siRNA delivery. *J. Control. Release* 2013; 171(3), 296–307.

28. Gujrati M, Vaidya A, Lu ZR. Multifunctional pH-sensitive amino lipids for siRNA delivery. *Bioconjug. Chem.* 2016; 27(1), 19–35.

29. Wang ZL, Xu R, Lu ZR. A peptide-targeted delivery system with pH-sensitive amphiphilic cell membrane disruption for efficient receptor-mediated siRNA delivery. *J. Control. Release* 2009; 134(3), 207–213.

30. Parvani JG, Gujrati MD, Mack MA, *et al.* Silencing beta3 integrin by targeted ECO/siRNA nanoparticles inhibits EMT and metastasis of triple-negative breast cancer. *Cancer Res.* 2015; 75(11), 2316–2325.

31. Gilleron J, Querbes W, Zeigerer A, *et al.* Image-based analysis of lipid nanoparticle-mediated siRNA delivery, intracellular trafficking and endosomal escape. *Nat. Biotechnol.* 2013; 31(7), 638–646.

32. Wang XL, Nguyen T, Gillespie D, *et al.* A multifunctional and reversibly polymerizable carrier for efficient siRNA delivery. *Biomaterials* 2008; 29(1), 15–22.

33. Xu R, Wang XL, Lu ZR. New amphiphilic carriers forming pH-sensitive nanoparticles for nucleic acid delivery. *Langmuir* 2010; 26(17), 13874–13882.

34. Xu R, Lu ZR. Design, synthesis and evaluation of spermine-based pH-sensitive amphiphilic gene delivery systems: multifunctional non-viral gene carriers. *Sci. China Chem.* 2011; 54(2), 359–368.

35. Sun D, Sun Z, Jiang H, *et al.* Synthesis and evaluation of pH-sensitive multifunctional lipids for efficient delivery of CRISPR/Cas9 in gene editing. *Bioconjug. Chem.* 2019; 30(3), 667–678.

36. Wang XL, Xu R, Wu X, *et al.* Targeted systemic delivery of a therapeutic siRNA with a multifunctional carrier controls tumor proliferation in mice. *Mol. Pharm.* 2009; 6(3), 738–746.

37. Sun D, Sahu B, Gao S, *et al.* Targeted multifunctional lipid ECO plasmid DNA nanoparticles as efficient non-viral gene therapy for Leber's congenital amaurosis. *Mol. Ther. Nucleic Acids* 2017; 7, 42–52.

38. Schilb AL, Ayat NR, Vaidya AM, *et al.* Efficacy of targeted ECO/miR-200c nanoparticles for modulating tumor microenvironment and treating triple negative breast cancer as non-invasively monitored by mr molecular imaging. *Pharm. Res.* 2021; 38(8), 1405–1418.

39. Vaidya AM,Sun Z, Ayat N, *et al.* Systemic delivery of tumor-targeting siRNA nanoparticles against an oncogenic LncRNA facilitates effective triple-negative breast cancer therapy. *Bioconjug. Chem.* 2019; 30(3), 907–919.

40. Nicolescu C, Kim J, Sun D, *et al.* Assessment of the efficacy of the combination of RNAi of lncRNA DANCR with chemotherapy to treat triple negative breast cancer using magnetic resonance molecular imaging. *Bioconjug. Chem.* 2024; 35(3), 381–388.

41. Wang XL, Jensen R, Lu ZR. A novel environment-sensitive biodegradable polydisulfide with protonatable pendants for nucleic acid delivery. *J. Control. Release* 2007; 120(3), 250–258.

42. Borovjagin VL, Vergara JA, McIntosh TJ. Morphology of the intermediate stages in the lamellar to hexagonal lipid phase transition. *J. Membr. Biol.* 1982; 69(3), 199–212.

43. Bentz J, Ellens H, Szoka FC. Destabilization of phosphatidylethanolamine-containing liposomes: hexagonal phase and asymmetric membranes. *Biochemistry* 1987; 26(8), 2105–2116.

44. Rupert LA, van Breemen JF, van Bruggen EF, *et al.* Calcium-induced fusion of didodecylphosphate vesicles: the lamellar to hexagonal II (HII) phase transition. *J. Membr. Biol.* 1987; 95(3), 255–263.

45. Chatterjee S, Kon E, Sharma P, *et al.* Endosomal escape: a bottleneck for LNP-mediated therapeutics. *Proc. Natl Acad. Sci. USA* 2024; 121(11), e2307800120.

46. Gandek TB, van der Koog L, Nagelkerke A. A comparison of cellular uptake mechanisms, delivery efficacy, and intracellular fate between liposomes and extracellular vesicles. *Adv. Healthc Mater.* 2023; 12(25), e2300319.

47. Gujrati M, Vaidya AM, Mack M, *et al.* Targeted dual pH-sensitive lipid ECO/siRNA self-assembly nanoparticles facilitate *in vivo* cytosolic sieIF4E delivery and overcome paclitaxel resistance in breast cancer therapy. *Adv Healthc Mater* 2016; 5(22), 2882–2895.

48. Ayat NR, Sun Z, Sun D, *et al.* Formulation of biocompatible targeted ECO/siRNA nanoparticles with long-term stability for clinical translation of RNAi. *Nucleic Acid Ther.* 2019; 29(4), 195–207.

49. Chung E, Reinaker K, Meyers R. Ethanol content of medications and its effect on blood alcohol concentration in pediatric patients. *J. Pediatr. Pharmacol. Ther.* 2024; 29(2), 188–194.

50. Nema S, Brendel RJ. Excipients and their role in approved injectable products: current usage and future directions. *PDA J. Pharm. Sci. Technol.* 2011; 65(3), 287–332.

51. Sun D, Sun W, Gao SQ, *et al.* Effective gene therapy of Stargardt disease with PEG-ECO/pGRK1-ABCA4-S/MAR nanoparticles. *Mol. Ther. Nucleic Acids* 2022; 29, 823–835.

52. Eldakhakhny B, Sutaih AM, Siddiqui MA, *et al.* Exploring the role of noncoding RNAs in cancer diagnosis, prognosis, and precision medicine. *Noncoding RNA Res.* 2024; 9(4), 1315–1323.

53. Benacka R, Szaboova D, Gulasova Z, *et al.* Non-coding RNAs in breast cancer: diagnostic and therapeutic implications. *Int. J. Mol. Sci.* 2024; 26(1), 127.

54. Wu D, Thompson LU, Comelli EM. MicroRNAs: a link between mammary gland development and breast cancer. *Int. J. Mol. Sci.* 2022; 23(24), 15978.

55. Balkrishna A, Mittal R, Bishayee A, *et al.* miRNA signatures affecting the survival outcome in distant metastasis of triple-negative breast cancer. *Biochem. Pharmacol.* 2025; 231, 116683.

56. Alavanda C, Dirimtekin E, Mortoglou M, *et al.* BRCA mutations and microRNA expression patterns in the peripheral blood of breast cancer patients. *ACS Omega* 2024; 9(15), 17217–17228.

57. Laney V, Hall R, Yuan X, *et al.* MR molecular image guided treatment of pancreatic cancer with targeted ECO/miR-200c nanoparticles in immunocompetent mouse tumor models. *Pharm. Res.* 2024; 41(9), 1811–1825.

58. Sun D, Schur RM, Lu ZR. A novel nonviral gene delivery system for treating Leber's congenital amaurosis. *Ther. Deliv.* 2017; 8(10), 823–826.

59. Sun D, Schur RM, Sears AE, *et al.* Stable retinoid analogue targeted dual pH-sensitive smart lipid ECO/pDNA nanoparticles for specific gene delivery in the retinal pigment epithelium. *ACS Appl. Bio. Mater.* 2020; 3(5), 3078–3086.

60. Sun D, Schur RM, Sears AE, *et al.* Non-viral gene therapy for Stargardt disease with ECO/pRHO-ABCA4 self-assembled nanoparticles. *Mol. Ther.* 2020; 28(1), 293–303.

61. Sun D, Sun W, Gao SQ, *et al.* Formulation and efficacy of ECO/pRHO-ABCA4-SV40 nanoparticles for nonviral gene therapy of Stargardt disease in a mouse model. *J. Control. Release* 2021; 330, 329–340.

62. Sun D, Sun W, Gao SQ, *et al.* Intravitreal delivery of PEGylated-ECO plasmid DNA nanoparticles for gene therapy of stargardt disease. *Pharm. Res.* 2024; 41(4), 807–817.

AFFILIATIONS

Victoria EA Laney, Department of Biomedical Engineering, Case Western Reserve University, Cleveland, OH, USA and Department of Biomedical Engineering, University of Illinois Chicago, Chicago, IL, USA

Zheng-Rong Lu, Department of Biomedical Engineering, Case Western Reserve University, Cleveland, OH, USA and Case Comprehensive Cancer Center, Case Western Reserve University, Cleveland, OH, USA

AUTHORSHIP & CONFLICT OF INTEREST

Contributions: The named authors take responsibility for the integrity of the work as a whole, and have given their approval for this version to be published.

Acknowledgements: None.

Disclosure and potential conflicts of interest: The authors have the following patents: US Patent 10,792,374, US 11,129,845, US Patent 11,407,786, US Patent 12,060,318.

Funding declaration: This research was supported in part by National Cancer Institute (NCI) grants from the National Institutes of Health (NIH), including R01 CA194518 (completed), R01 CA235152, and R01 CA297621, as well as an NCI CURE Supplemental Award under the R01 CA235152 parent grant. Additional funding was provided by the Gund-Harrington Scholars Award from the Harrington Discovery Institute and the Foundation Fighting Blindness (completed), a grant from the Case-Coulter Translational Research Partnership and OhioJobs, and support from Emily's Entourage.

ARTICLE & COPYRIGHT INFORMATION

Article source: Invited; externally peer reviewed.

Submitted for peer review: Apr 23, 2025.

Revised manuscript received: Jun 23, 2025.

Publication date: Jul 21, 2025.

NUCLEIC ACID INSIGHTS

FORMULATION AND DELIVERY
GETTING BEYOND THE LIVER

SPOTLIGHT

AI-driven modular platform for peptide dendrimer lipid nanocarriers: streamlining and accelerating precision nucleic acid delivery

Tristan Henser-Brownhill and Albert Kwok

VIEWPOINT

"AI-driven methodologies promise to accelerate innovation, guiding researchers toward the next generation of highly efficient, precision-engineered nanocarriers."

Nucleic Acid Insights 2025; 2(6), 105–108 · DOI: 10.18609/nuc.2025.017

Lipid-based nanocarriers, particularly lipid nanoparticles (LNPs), have transformed the landscape of nucleic acid delivery, finding success in mRNA vaccines and gene therapies. However, these delivery systems remain constrained by their inherent

liver tropism, limiting broader therapeutic applications. Recent advances in modular peptide dendrimer lipid hybrids and artificial intelligence (AI)-driven screening techniques are now reshaping the field, offering greater precision and efficiency in targeting delivery systems beyond the liver.

OVERCOMING LIVER TROPISM IN LIPID-BASED NANOCARRIERS

Traditional LNPs naturally accumulate in the liver due to their interaction with plasma proteins, such as apolipoprotein E (ApoE), which facilitates hepatocyte uptake via low-density lipoprotein (LDL) receptors [1]. While beneficial for liver-targeted therapies, this characteristic poses a significant hurdle for delivering nucleic acids to extrahepatic tissues. To address this, researchers have explored structural modifications, including surface charge manipulation and ligand-based targeting.

A novel approach gaining traction is the integration of dendrimers, made of either synthetic polymers [2,3] or more biocompatible branched peptides [4,5], into lipid based nanocarriers. Pioneered by Kwok *et al.*, peptide dendrimer lipid systems leverage the highly branched and tunable nature of peptide dendrimers to enhance transfection efficiency [4]. By adjusting the charge distribution, hydrophobicity, and targeting properties of the peptide dendrimer lipid systems, researchers can influence the biodistribution of nanocarriers, opening pathways for targeted delivery to tissues such as the lungs, spleen, and central nervous system.

THE ADVANTAGES OF A MODULAR PEPTIDE DENDRIMER SYSTEM

The peptide dendrimer lipid delivery system offers distinct advantages over conventional lipid based nanocarriers due to their modular nature. Unlike traditional LNPs, where targeting capabilities often rely on external ligand modifications, peptide dendrimer lipid systems allow for intrinsic control over charge, hydrophilicity, and targeting affinity.

Key benefits of this approach include:

- Enhanced stability and controlled release. Peptide dendrimers provide greater structural integrity, preventing premature degradation and ensuring a more controlled release of nucleic acid payloads.
- Tunable surface chemistry. By designing peptide dendrimers with specific amino acid residues, researchers can fine-tune interactions with biological barriers, reducing off-target effects.
- Improved cellular uptake and endosomal escape. Peptide dendrimers can be engineered to guide specific endocytotic pathways and selectively target different cell receptors. It can also enhance endosomal escape, a major bottleneck in nucleic acid delivery, thereby increasing transfection efficiency.

These properties make peptide dendrimer lipid hybrid carriers a promising alternative for nucleic acid-based therapeutics, particularly in cases requiring targeted gene editing or immunotherapy applications beyond hepatic tissues.

AI AND ML DRIVEN NANOCARRIER DESIGN

The rapid evolution of AI and machine learning (ML) is further accelerating progress in nanocarrier development. Henser-Brownhill et al. have demonstrated the power of AI-driven screening by computationally modeling over 4.5 million potential peptide dendrimer lipid formulations to optimize their efficacy [6]. AI-powered simulations allow researchers to predict the key physicochemical and behavioural properties of nanocarriers that affect their manufacturability and delivery efficacy before

experimental validation in the lab, significantly reducing development time and costs.

Moreover, ML algorithms are enhancing the rational design of nanocarriers by identifying patterns in physicochemical properties that correlate with successful delivery outcomes. By integrating AI-driven predictions with high-throughput experimentation, scientists can refine carrier compositions, optimize nanoparticle stability, and tailor targeting capabilities with unprecedented speed and precision.

THE FUTURE OF NUCLEIC ACID DELIVERY

To ensure the continued expansion of nucleic acid-based therapies in treating a broader range of life-threatening diseases, overcoming delivery barriers remains paramount. The advent of peptide dendrimer lipid hybrids represents a critical step forward, providing a modular, tunable approach to targeted delivery. Meanwhile, AI-driven methodologies promise to accelerate innovation, guiding researchers toward the next generation of highly efficient, precision-engineered nanocarriers.

With these advances, the field stands at the brink of a new era in precision medicine—one where intelligent nanocarriers can be designed and optimized computationally, ensuring safer and more effective nucleic acid therapies for a wider range of diseases.

REFERENCES

1. Sato Y, Kinami Y, Hashiba K, Harashima H. Different kinetics for the hepatic uptake of lipid nanoparticles between the apolipoprotein E/low density lipoprotein receptor and the N-acetyl-d-galactosamine/asialoglycoprotein receptor pathway. *J. Contr. Release* 2020; 322, 217–226.
2. Cheng Q, Wei T, Jia Y, Farbiak L, *et al*. Dendrimer-based lipid nanoparticles deliver therapeutic FAH mRNA to normalize liver function and extend survival in a mouse model of hepatorenal tyrosinemia type I. *Adv. Mater.* 2018; 30(52), 1805308.
3. Farbiak L, Cheng Q, Wei T, Álvarez-Benedicto E, *et al*. All-in-one dendrimer-based lipid nanoparticles enable precise HDR-mediated gene editing in vivo. *Adv. Mater.* 2021; 33(30), 2006619.
4. Kwok A, Eggimann GA, Reymond JL, Darbre T, Hollfelder F. Peptide dendrimer/lipid hybrid systems are efficient DNA transfection reagents: structure–activity relationships highlight the role of charge distribution across dendrimer generations. *ACS Nano* 2013; 7(5), 4668–4682.
5. Kwok A, Eggimann GA, Heitz M, Reymond, JL, *et al*. Efficient transfection of siRNA by peptide dendrimer–lipid conjugates. *ChemBioChem* 2016; 17(23), 2223–2229.
6. Henser-Brownhill T, Martin L, Samangouei P, Ladak A, *et al*. *In silico* screening accelerates nanocarrier design for efficient mRNA delivery. *Adv. Sci.* 2014; 11(30), 2401935.

BIOGRAPHIES

Tristan Henser-Brownhill is a Machine Learning Engineer and Computational Biologist at Nuntius Therapeutics, where he leads the design and deployment of scalable ML and bioinformatics solutions to accelerate gene therapy research. He holds a PhD in Computational Biology from the University of Manchester, Manchester, UK, where he applied machine learning to the analysis of data from novel imaging technologies. Tristan has held research

positions at institutions including Cancer Research UK, Manchester, UK and the Francis Crick Institute, London, UK, contributing to high-impact publications and translational discoveries in cancer epigenomics and CRISPR technology.

Tristan Henser-Brownhill PhD, Machine Learning Engineer and Computational Biologist, Nuntius Therapeutics, London, UK

Albert Kwok is the Co-founder and Chief Scientific Officer of Nuntius Therapeutics, a venture-backed biotech company pioneering cutting-edge nucleic acid therapies. With over 20 years of experience in the field, Albert earned his PhD from University College London, London, UK and held academic positions at the University of Cambridge, Cambridge, UK before developing RNA medicines at MiNA Therapeutics, London, UK. Driven by a deep commitment to scientific discovery and real-world impact, Albert continues to drive the development of innovative therapies that can transform the lives of patients worldwide.

Albert Kwok PhD, Co-founder and Chief Scientific Officer, Nuntius Therapeutics, London, UK

AUTHORSHIP & CONFLICT OF INTEREST

Contributions: The named authors take responsibility for the integrity of the work as a whole, and has given their approval for this version to be published.

Acknowledgements: None.

Disclosure and potential conflicts of interest: The authors have published a paper at *Advanced Science* on their machine learning work and Albert Kwok has presented their work at an EU RNA conference. They also have patents pending related to this article. Albert Kwok is co-founder, director, and a stock holder of Nuntius Therapeutics.

Funding declaration: The authors have received funding from Nuntius Therapeutics.

ARTICLE & COPYRIGHT INFORMATION

Article source: Invited.

Revised manuscript received: Mar 31, 2025.

Publication date: May 22, 2025.

NUCLEIC ACID INSIGHTS

INNOVATOR INSIGHT

A scalable purification strategy for removal of dsRNA byproducts following IVT RNA production

Nathaniel Clark

The presence of double-stranded RNA byproducts in *in vitro* transcription reactions is a significant concern in the production of synthetic mRNA therapeutics due to their potential to trigger unwanted innate immune responses. This article presents the development, validation, and application of a dsRNA-specific affinity resin using affinity ligand technology coupled with a macroporous base bead.

Nucleic Acid Insights 2025; 2(5), 117–129 · DOI: 10.18609/nuc.2025.018

CHALLENGES OF dsRNA BYPRODUCTS IN mRNA THERAPEUTIC PRODUCTION

Although dsRNA species are typically present at very low levels, they are highly immunogenic. Due to their low abundance, real-time monitoring of dsRNA during the manufacturing process is not currently feasible. Additionally, upstream control of dsRNA is difficult, and there is a lack of regulatory consensus regarding acceptable dsRNA levels in final mRNA products.

A recent study demonstrated that dsRNA levels as low as 0.0006% can elicit a measurable immunogenic response, while a dsRNA level of 0.00007% did not1. These observations support the hypothesis that minimizing dsRNA content is critical to decreasing adverse immune responses, which may allow for higher dosing and more effective response to mRNA-based therapeutics.

Another major limitation in the field is the lack of quantitative and size-specific characterization methods for dsRNA. Current assays primarily rely on bulk immunoreactivity measurements, which provide limited insights into the size distribution or relative immunogenic potential of distinct dsRNA species. Further, dsRNA molecules are challenging to remove during downstream processing. They are similar in size and structure to the target mRNA, copurifying during oligo-dT affinity chromatography, and are not effectively separated by tangential flow filtration (TFF). This indicates that their biophysical properties closely resemble those of therapeutic mRNA.

FIGURE 1

Immuno-northern blot assay to assess dsRNA size distribution.

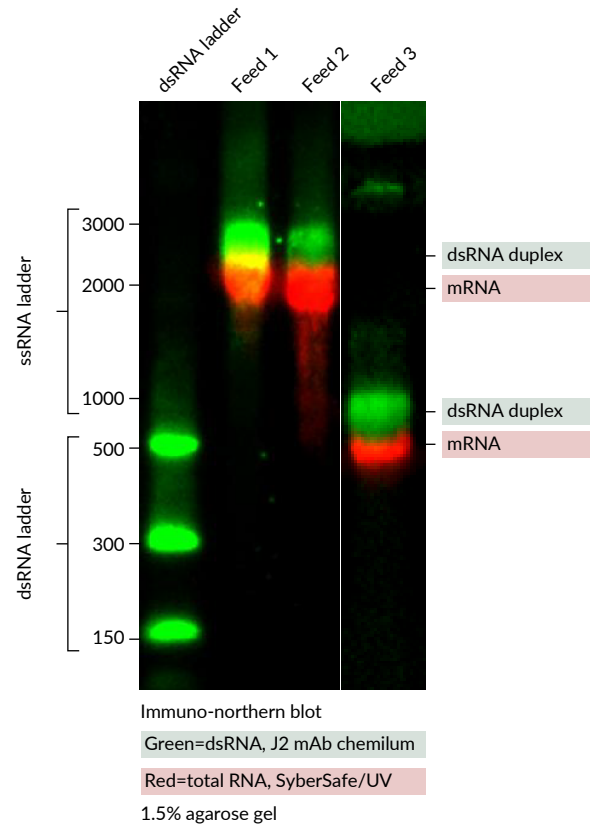

APPLICATION OF IMMUNO-NORTHERN BLOT TO DETERMINE dsRNA BYPRODUCT SIZE

During the development of dsRNA-specific affinity resin, a critical consideration was the size of the dsRNA species that must be removed from mRNA preparation. Despite extensive speculation in literature, ranging from small abortive transcripts to loopback hairpin structures, there is no clear consensus regarding the size distribution of dsRNA byproducts. To address this, a direct analytical method was required to characterize the dsRNA species present in mRNA production streams.

To this end, an immuno-northern blot assay was developed to assess dsRNA size distribution [2]. This technique is analogous to a Western blot but is applied to RNA using the J2-specific monoclonal antibody. In this method, RNA samples are resolved on an agarose gel and stained to visualize total RNA content. Subsequent transfer to a membrane and probing with the J2 antibody allows for specific detection of dsRNA species. As illustrated in **Figure 1**, total mRNA stain appears in red, while dsRNA-specific signals are detected using immunostaining.

Analysis of three representative feedstocks showed that the majority of dsRNA byproducts are larger in size relative to the primary mRNA transcript. These findings suggest that many of these dsRNAs may result from extension of the 3′ hairpin structures, generating a dsRNA with twice the molecular mass of the mRNA transcript. For example, a full-length luciferase dsRNA would have a molecular mass of approximately 1,100 kD, highlighting the large size of the target contaminants.

QUANTIFICATION OF dsRNA LEVELS IN mRNA PREPARATIONS

Accurate quantification of dsRNA byproducts represents another critical challenge in the development and quality control (QC) of mRNA therapeutics. While the J2 immuno-dot blot assay is widely used across academic and industrial settings due to its simplicity and convenience, it is inherently qualitative. As such, it is difficult to compare results across experiments or between different days unless all samples are processed on the same membrane, limiting its utility for longitudinal studies or process optimization.

To support consistent evaluation of dsRNA levels during prototype testing and experimental development, a more robust and quantitative assay was required. Several ELISA kits were found and tested, and among these was the Vazyme EasyAna dsRNA ELISA kit. This showed significant reproducibility, high sensitivity, and compatibility with high-salt buffer systems commonly used in RNA purification workflows. Importantly, no matrix effects were

FIGURE 2

Comparison of J2 dot blot and quantitative ELISA to assess dsRNA levels in mRNA preparations.

Comparison of J2 dot blot and quantitative ELISA				
µg mRNA		% dsRNA equivalent	(dsRNA) µg/mL	CV (%)
1		5	0.49	4
0.3		1.7	0.17	7
0.1		0.54	0.055	4
0.03		0.18	0.018	4
0.01		0.060	0.0060	4
0.004		0.019	0.0019	1
0.001		0.0065	0.0007	4
0.0004		0.0022	0.0002	0

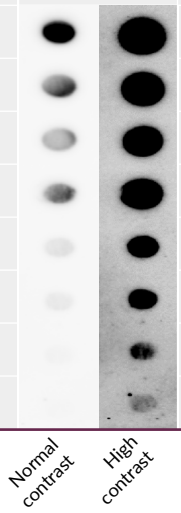

observed under these conditions, eliminating the need to buffer exchange samples prior to analysis.

This quantitative assay significantly enhanced the ability to track and optimize dsRNA removal throughout process development. As shown in **Figure 2**, the ELISA results were consistent with those obtained from the J2 dot blot assay, supporting the reliability and accuracy of this method for dsRNA quantification. Furthermore, the ELISA gave very consistent results when the same samples were analyzed on different days, and by different analysts.

DESIGN OF HIGH-AFFINITY LIGANDS FOR dsRNA BYPRODUCT REMOVAL

To develop high-affinity ligands capable of selectively capturing dsRNA byproducts, the AVIPure® technology platform was employed. AVIPure scaffolds are composed of small, highly stable proteins and peptides that are identified entirely through *in vitro* selection processes, without the need for animal immunization. These scaffolds are not antibodies. AVIPure ligands offer high binding affinities and excellent chemical

FIGURE 3

Electron microscopy of DuloCore base bead affinity resin.

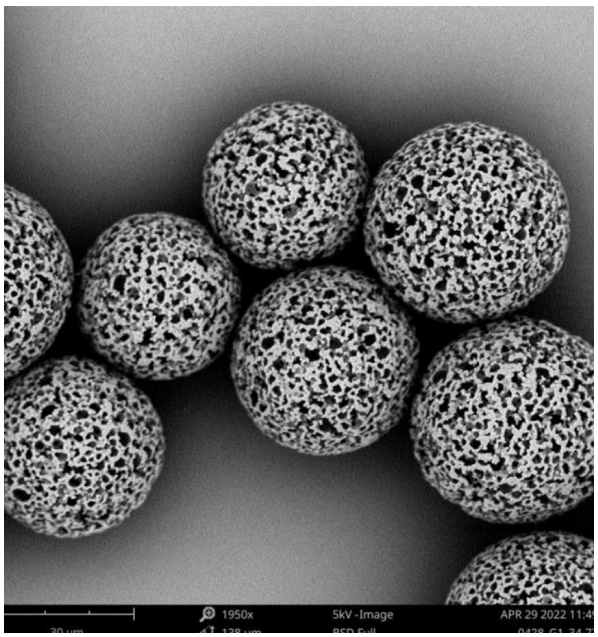

FIGURE 4

(A) Size range of dsRNA fragments captured by affinity resin over a 1.8 kbp luciferase duplex and dsRNA ladder of 500–80 bp. (B) dsRNA and mRNA binding of affinity resin compared to cellulose.

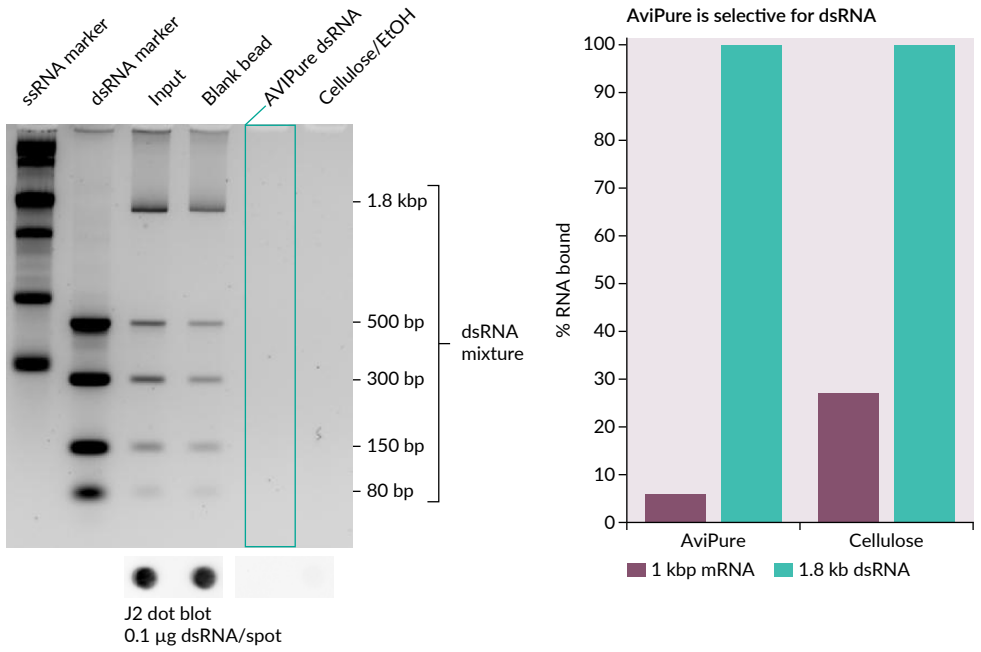

stability in sodium hydroxide (NaOH), which is commonly used for column regeneration and sanitization. As a result, affinity resins functionalized with AVIPure ligands exhibit excellent cleanability, durability, and cost-effectiveness.

An equally critical component of the affinity resin is the base matrix. Given the high MW and size of dsRNA contaminants identified during characterization, the DuloCore™ base bead was selected. The resin features a distinctive macroporous architecture, as shown in the electron micrograph in **Figure 3**, with large through-pores that enable superior mass transfer and facilitate rapid flow rates. These properties make the bead particularly well-suited for capturing large biomolecules such as dsRNA.

In addition to its high binding efficiency, the bead format allows for scalable column design and robust operation. The resin supports high flow rates, can accommodate reverse-flow cleaning, and tolerates aggressive cleaning protocols—features that are especially advantageous in the context of *in vitro* transcription processes.

VALIDATION OF dsRNA BYPRODUCT REMOVAL USING AFFINITY RESIN

To validate the performance of the dsRNA-specific affinity resin, a capacity breakthrough assay was conducted using a purified 500 bp dsRNA. The assay measures binding capacity at the 10% breakthrough point, yielding an average dynamic binding capacity of approximately 0.5 g of dsRNA per liter of resin. A recommended minimum loading of 10 g of total RNA per liter of resin is suggested for practical applications to ensure both good recovery and avoid breakthrough. Higher amounts may be loaded when the dsRNA content of the feed is lower. The resin is compatible with various RNA modalities, including circular RNA, self-amplifying RNA, and

FIGURE 5

Gel electrophoresis of GFP mRNA before and after AVIPure purification.

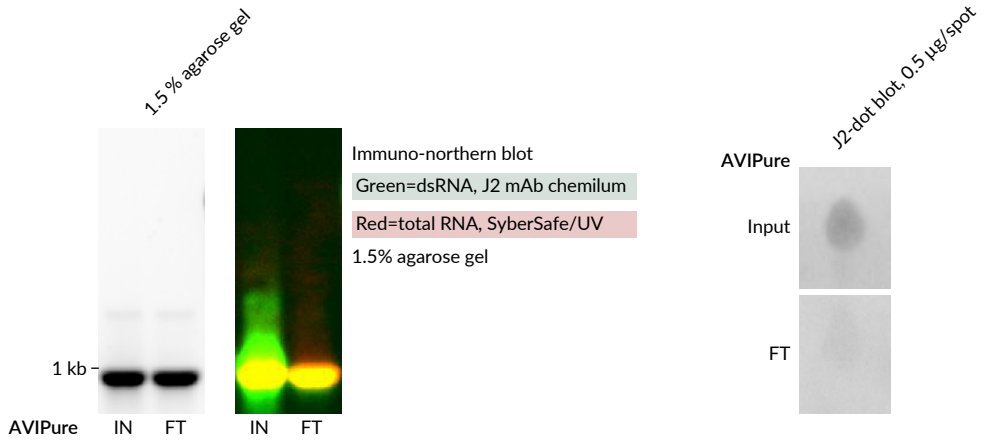

Sample	Ratio of dsRNA to ssRNA (%) Vazyme ELISA data		Fold reduction	Log reduction
	Input	AVIPure		
Ald Dasher GFP	0.1269	0.0001	1269	3.1

other transcribed single-stranded RNA formats.

A common inquiry from end-users concerns the size range of dsRNA fragments that the resin can effectively capture. Experimental data demonstrate that the resin binds a broad range of dsRNA sizes. In **Figure 4A**, a 1.8 kbp luciferase duplex and a dsRNA ladder of 500–80 bp were efficiently captured by the resin. Additional data confirmed binding of fragments as small as 21 bp [1].

While immuno-northern blot analyses indicate that most dsRNA byproducts are large, it is notable that the resin can also remove smaller fragments. A comparison of dsRNA and mRNA binding further confirms that the affinity resin exhibits strong selectivity for dsRNA, with minimal retention of the target mRNA, as shown in **Figure 4B**.

Further validation was performed using a green fluorescent protein (GFP) mRNA, which contained only transcription-derived dsRNA impurities. **Figure 5** shows the gel electrophoresis of samples before and after AVIPure purification, which revealed no detectable change in RNA integrity, as expected due to the low dsRNA abundance of approximately 0.1%. However, immuno-northern blot analysis showed complete loss of dsRNA signal following purification. Similarly, dot blot results confirmed this removal, although the semi-quantitative nature of this assay limited interpretation of removal efficiency.

Quantitative analysis using a dsRNA-specific ELISA indicated a 1,269-fold reduction in dsRNA content, from 0.12 to 0.0001%, representing an approximate 3.1-log decrease. Although low, this residual level was still above the assay's lower limit of quantification (LOQ).

PROCESS OPTIMIZATION OF dsRNA BYPRODUCT REMOVAL

To support process optimization, a high-throughput 96-well filter plate format was employed. In this assay, AVIPure resin was incubated with RNA under varying pH and sodium chloride (NaCl) concentrations. This can be seen in **Figure 6**, where

columns of the plate represented different pH values, while rows varied in NaCl concentration. The left half of the plate contained AVIPure resin; the right half served as a no-resin control.

Results demonstrated that under neutral pH conditions, increasing salt concentration, particularly in the 0.4–0.75 M NaCl range, enhanced dsRNA removal. Corresponding immuno-northern blot analysis confirmed a marked reduction in dsRNA signal in AVIPure-treated samples compared to controls.

Finally, the resin was shown to be stable in both NaOH and guanidine hydrochloride (GdnHCl). For R&D applications, GdnHCl may be used to elute bound dsRNA, preserving the material for downstream analysis or assay development. For manufacturing applications, regeneration with 0.1 M NaOH is recommended (dsRNA cannot be recovered from 0.1 M NaOH due to base-catalyzed hydrolysis). In simulated CIP studies, the resin retained full capacity following 10 simulated 15-minute cycles (2.5-hour total exposure to NaOH). Higher stringency cleaning with 0.5 M NaOH for 30 minutes was also feasible, with capacity remaining consistent with that of resin prior to exposure.

CASE STUDIES: PURIFICATION OF FIREFLY LUCIFERASE dsRNA AND CYCLING PERFORMANCE WITH GdnHCl ELUTION

To demonstrate the real-world application of the affinity resin, case studies were conducted using firefly luciferase RNA synthesized via a commercial IVT kit. This RNA contained approximately 0.7% dsRNA, as determined by ELISA.

In the first experiment, shown in **Figure 7A**, the chromatogram illustrates the purification process. The RNA sample was applied to the AVIPure column using a pump. As this is not a bind-elute format, the mRNA in the flow-through is somewhat diluted. To mitigate potential losses from peak broadening and nonspecific interactions, a minimum loading of 10 mg of RNA per mL column volume is recommended. This ensures improved mRNA recovery and performance consistency.

Following the sample application and buffer chase, bound dsRNA was eluted

FIGURE 6

High-throughput 96-well filter plate with AVIPure resin incubated with RNA under varying pH and NaCl concentrations.

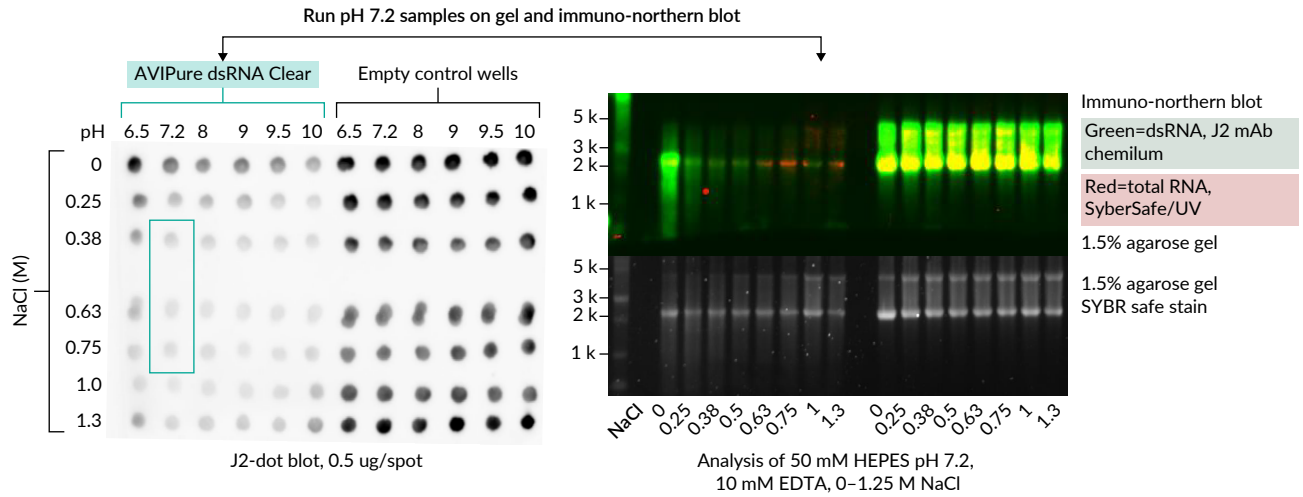

FIGURE 7

Analysis of dsRNA-enriched eluates in (A) chromatograph of purification process, (B) ELISA sample application and buffer chase, (C) dot blot analysis, and (D) immuno-northern blot concentrations.

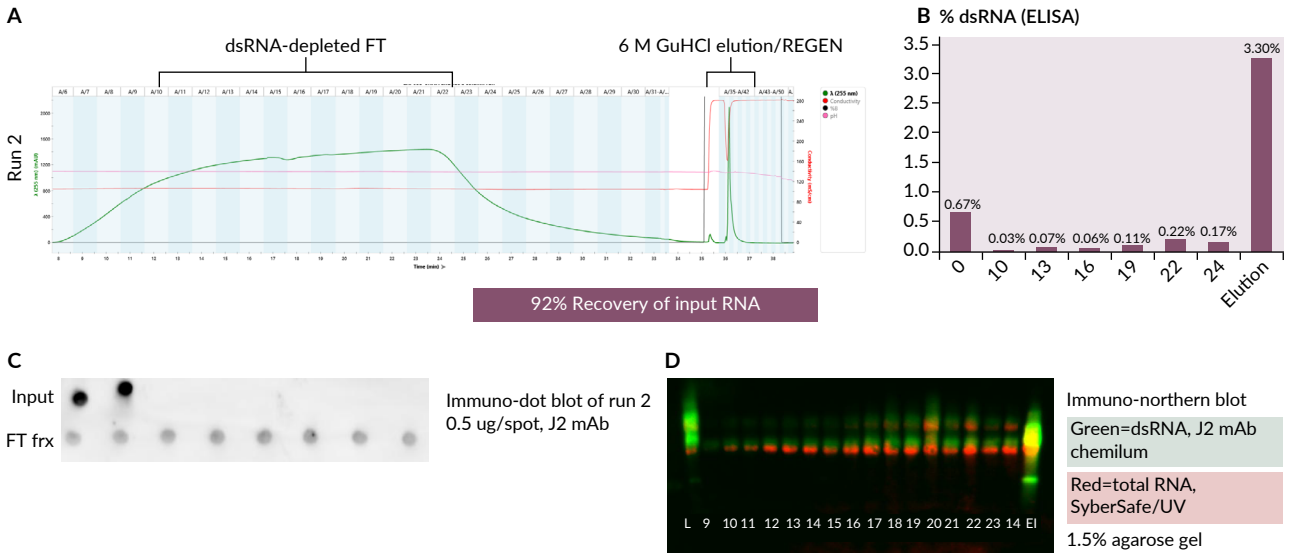

FIGURE 8

Luciferase RNA purification repeated over five consecutive runs using GndHCl for elution and CIP.

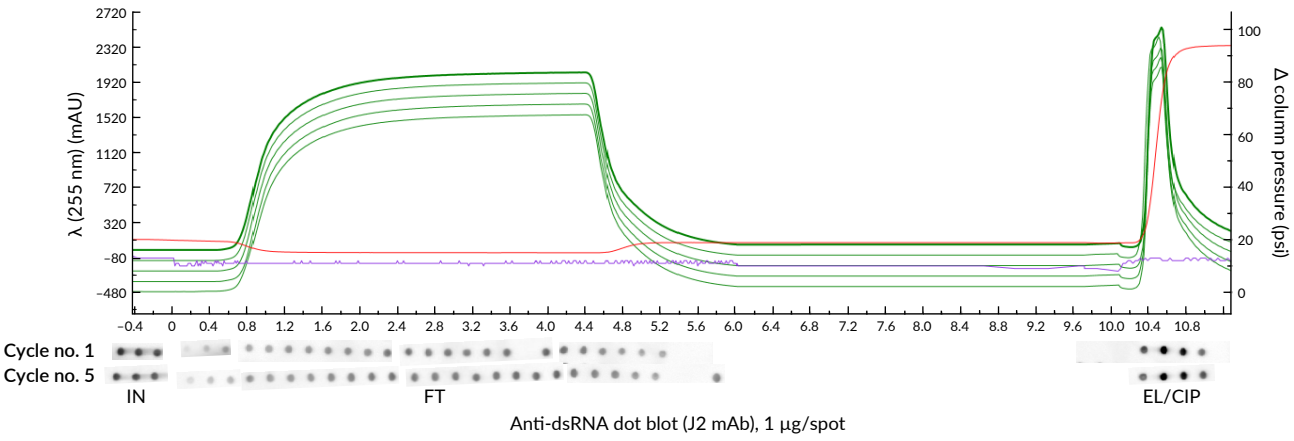

	Run 1	Run 2	Run 3	Run 4	Run 5
% FT	88%	87%	86%	91%	90%
% elut	13%	11%	10%	10%	10%
% mass balance	102%	98%	96%	101%	100%

using 6 M GdnHCl. A sharp elution peak was observed. ELISA quantification of dsRNA, shown in **Figure 7B**, indicated a 4- to 10-fold reduction in the flow-through and significant enrichment of dsRNA in the eluate. Although luciferase RNA typically

FIGURE 9

Purification performance of affinity resin with agarose gel electrophoresis.

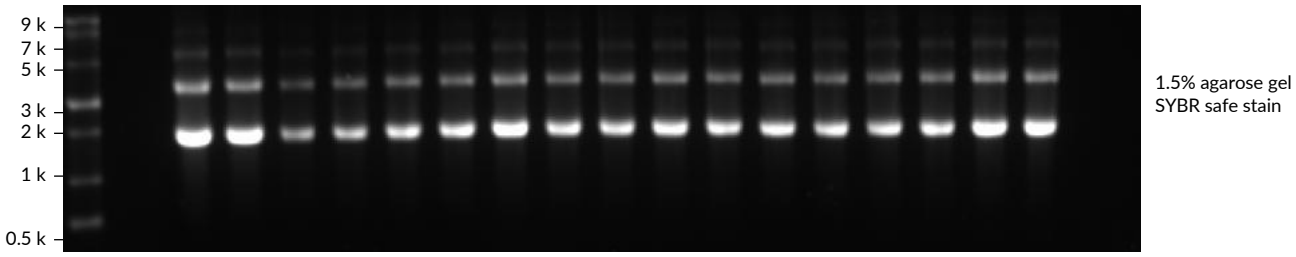

exhibits more modest dsRNA removal compared to other templates such as GFP, this result remains within the expected range for this template type.

Dot blot analysis, **Figure 7C**, confirmed a clear decrease in dsRNA signal post-purification. Immuno-northern blotting, **Figure 7D**, provided additional insight. The load sample exhibited a broad green smear indicative of diverse, large dsRNA species. This signal was markedly reduced in the flow-through, with only faint residual signal, possibly attributable to background. Notably, the elution fraction revealed the presence of distinct dsRNA bands, including a prominent band around 500 bp that was not visible in the original load. This result demonstrates the column's capacity to enrich low-abundance dsRNA species, enabling their detection with common analytical techniques.

In a follow-up cycling study, the same luciferase RNA purification was repeated over five consecutive runs using GndHCl for both elution and CIP, as seen in **Figure 8**.

Dot blot analysis from cycles 1 and 5 showed no degradation in performance, indicating the resin's robustness and stability under repeated guanidine exposure. mRNA recovery remained consistent at approximately 90% across all cycles, with good mass balance observed throughout the experiment. These studies highlight the practical utility, selectivity, and reusability of the AVIPure resin for dsRNA removal in mRNA manufacturing workflows.

CASE STUDY: COLUMN RUN WITH HIGHLY STRUCTURED mRNA

This case study highlights the purification performance of the affinity resin when applied to a particularly challenging sample—an mRNA with extensive secondary and tertiary structure. The agarose gel electrophoresis analysis, **Figure 9**, revealed the presence of multiple bands beyond the expected monomeric transcript. Notably, distinct bands appeared at approximately two and three times the primary transcript size, forming a ladder-like pattern indicative of intermolecular hybridization or multimeric species. These species are likely the result of interstrand duplex formation driven by the transcript's inherent structural motifs.

Following purification, analysis by immuno-dot blot showed minimal visual difference between the input and flow-through samples, suggesting limited dsRNA removal. Similarly, ELISA quantification reported no measurable reduction in dsRNA content, raising initial concerns about the resin's effectiveness with this feed material.

However, a subsequent immuno-northern blot, **Figure 10**, revealed a strikingly different result. The input lanes displayed heavy smearing characteristic of dsRNA byproducts, while the flow-through fractions showed complete clearance of this signal. This divergence among analytical methods underscores

FIGURE 10

Immuno-northern blotting of highly structured mRNA to assess the purification performance of affinity resin.

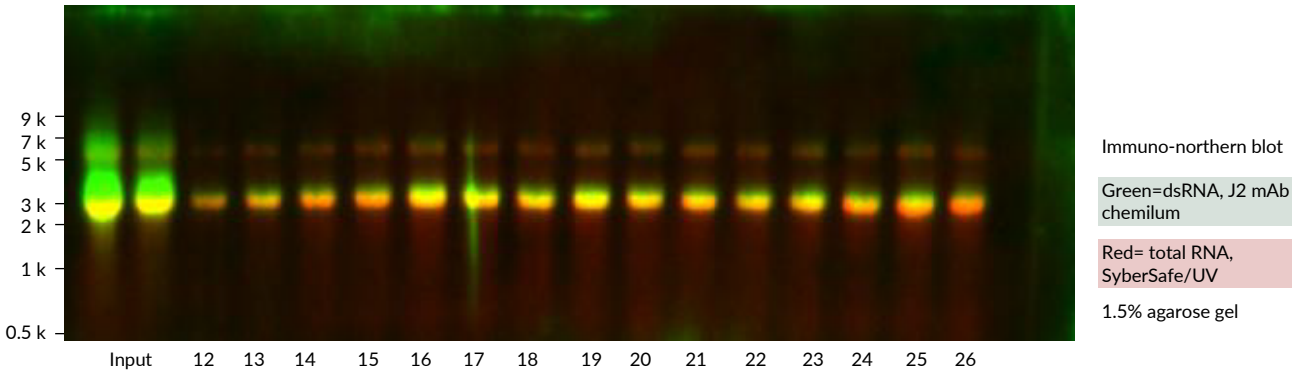

the limitations of relying on a single assay, particularly when working with structured or atypical RNA samples. In this instance, immuno-northern blotting provided the most accurate picture of dsRNA removal.

Evaluation by the collaborator using their in-house analysis confirmed that AVIPure did remove the dsRNA, reinforcing the conclusion that the observed discrepancies were due to analytical artifacts rather than process failure. Among the 30 RNA samples evaluated during product development, approximately 80% responded predictably and purified well using a standard oligo-dT-compatible binding buffer containing approximately 0.7 M salt. The remaining 20%, including this structured RNA and luciferase RNA, posed greater analytical and processing challenges.

These structured transcripts often display laddering on native gels and exhibit signs of heterogeneity, such as pre-peak shoulders in high-performance size exclusion chromatography, indicating polydispersity and the presence of higher-order species. Such structural complexity can reduce mass transfer efficiency and may affect ligand interaction, even if the resin itself retains its selectivity.

In this case study, the native gel profiles of the flow-through samples retained both the monomer and dimer bands, indicating that the resin does not indiscriminately bind all structured RNA. Rather, it distinguishes between true dsRNA, characterized by long, uninterrupted helices, and more localized structural elements typical of native mRNAs, which usually involve hairpins or duplexes of only 5–10 bp. This functional discrimination likely arises from the ligand's requirement for extended helical binding regions, enabling selective removal of long dsRNA contaminants while preserving structured single-stranded mRNAs. This case illustrates not only the effectiveness of AVIPure in handling highly structured transcripts, but also the importance of comprehensive and orthogonal analytical methods to accurately assess purification outcomes.

SUMMARY

Developing a dsRNA affinity resin required careful analysis of the size and nature of dsRNA byproducts. Data from immuno-northern blots, ELISA, and dot blot assays established dsRNA sizes, abundance, and structural features, information which guided the development of AVIPure dsRNA Clear affinity resin.

Case studies with firefly luciferase and highly structured mRNAs demonstrated the resin's ability to reduce dsRNA content while preserving mRNA integrity across

multiple cycles. Combining a high-affinity ligand and macroporous base bead provided robust, scalable performance, supporting improved mRNA product quality and advancing the manufacturing of RNA-based therapeutics for both R&D and manufacturing. This technology offers a scalable, selective, and reliable solution for reducing immunogenic dsRNA impurities in mRNA therapeutics.

Q&A

Nathaniel Clark

Q Our IVT process has been optimized to produce minimal levels of dsRNA. Is there any additional benefit to using this column for our mRNA?

NC The AVIPure column offers additional benefits even when dsRNA levels are already low. Based on extensive analysis of various RNA samples, the column has consistently achieved over 2-log reduction in dsRNA content, even from starting levels as low as 0.01%.

A clear correlation has been observed between reduced dsRNA content and decreased immunogenicity in cell-based assays. Importantly, there appears to be no lower threshold beyond which further dsRNA reduction ceases to be beneficial. Therefore, combining IVT optimization with AVIPure column purification provides the most effective strategy for minimizing dsRNA, reducing innate immune activation, and enabling optimal RNA dosing for a given therapeutic application.

Q Is dsRNA clear resin compatible with large self-amplifying RNA?

NC Yes, the dsRNA Clear resin is compatible with self-amplifying RNA (saRNA). Internally, RNAs up to approximately 5 kilobases in length have been tested, and external reports from users confirm effective performance with saRNA constructs. The convective flow properties of the macroporous base bead support rapid mass transfer, enabling efficient binding of double-stranded RNA species regardless of size. As a result, the resin demonstrates robust performance across a range of RNA lengths, including large saRNAs.

Nucleic Acid Insights 2025; 2(5), 117–129 · DOI: 10.18609/nuc.2025.018

Q Should the AVIPure column be used before or after mRNA purification on an oligo-dT column?

NC It is generally recommended to use the AVIPure column after oligo-dT purification. In most cases, optimal dsRNA removal has been observed when starting with oligo-dT-purified RNA. Although the AVIPure resin functions in a high-salt buffer, which may suggest compatibility with pre-oligo-dT use, there are practical considerations. IVT reaction mixtures can be complex, containing high RNA concentrations, precipitating divalent salts, and proprietary components that may interfere with dsRNA capture, and/or analytical assays. These feedstocks are often particulate-rich and may challenge resin performance or column lifetime. While some end-users have explored integrating AVIPure in-line with oligo-dT steps or placing it upstream, such approaches may introduce variables that complicate process development. For establishing a reliable baseline, it is advisable to first apply AVIPure purification to oligo-dT-purified RNA and subsequently assess upstream integration as needed.

Q How is the pure dsRNA standard generated for analytical validation?

NC Pure dsRNA standards are generated using a commercial IVT kit designed to produce both strands of a defined 500 bp sequence. This process yields high-quality, fully complementary dsRNA suitable for use in assay validation. For larger constructs such as luciferase dsRNA, both sense and antisense strands are independently transcribed and then annealed to form the duplex [2]. Overall, the procedure is straightforward and enables the production of well-characterized dsRNA controls for use in ELISA and other analytical techniques.

REFERENCES

1. Clark NE, Kozarski M, Asci SD, *et al.* Removal of dsRNA byproducts using affinity chromatography. *Mol. Ther. Nucleic Acids* 2025; 36(2), 102549.
2. Clark NE, Schraut MR, Winters RA, Kearns K, Scanlon TC. An immuno-northern technique to measure the size of dsRNA byproducts in *in vitro* transcribed RNA. *Electrophoresis* 2024; 45(17–18), 1546–1554.

BIOGRAPHY

Nathaniel Clark is a Downstream Scientist at Avitide, Lebanon, NH, USA, a Repligen company. He has a PhD in Biochemistry and Structural Biology from UMass Amherst, Amherst, MA, USA and moved into field of RNA as a postdoc at the University of Texas, Austin, TX, USA. At Avitide, he uses structural biology, protein engineering, and modeling to design novel affinity resins.

Nathaniel Clark PhD, Downstream Scientist, Downstream Development, Repligen

AUTHORSHIP & CONFLICT OF INTEREST

Contributions: The named author takes responsibility for the integrity of the work as a whole, and has given their approval for this version to be published.

Acknowledgements: None.

Disclosure and potential conflicts of interest: The author has no conflicts of interest.

Funding declaration: The author received no financial support for the research, authorship and/or publication of this article.

ARTICLE & COPYRIGHT INFORMATION

Article source: This article is based on a webinar, which can be found **here**.

Webinar recorded: Apr 9, 2025.

Revised manuscript received: May 28, 2025.

Publication date: Jul 25, 2025.

REPLIGEN

AVIPure® Affinity Resins

AVIPure® dsRNA for simple, reliable removal of dsRNA from mRNA

Remove dsRNA to <0.01% from post-IVT or post-oligo dT mRNA solutions

- Simple, flow through operation in aqueous buffer — dsRNA is captured, with no need to elute
- No solvents
- No cellulose
- Fast processing time

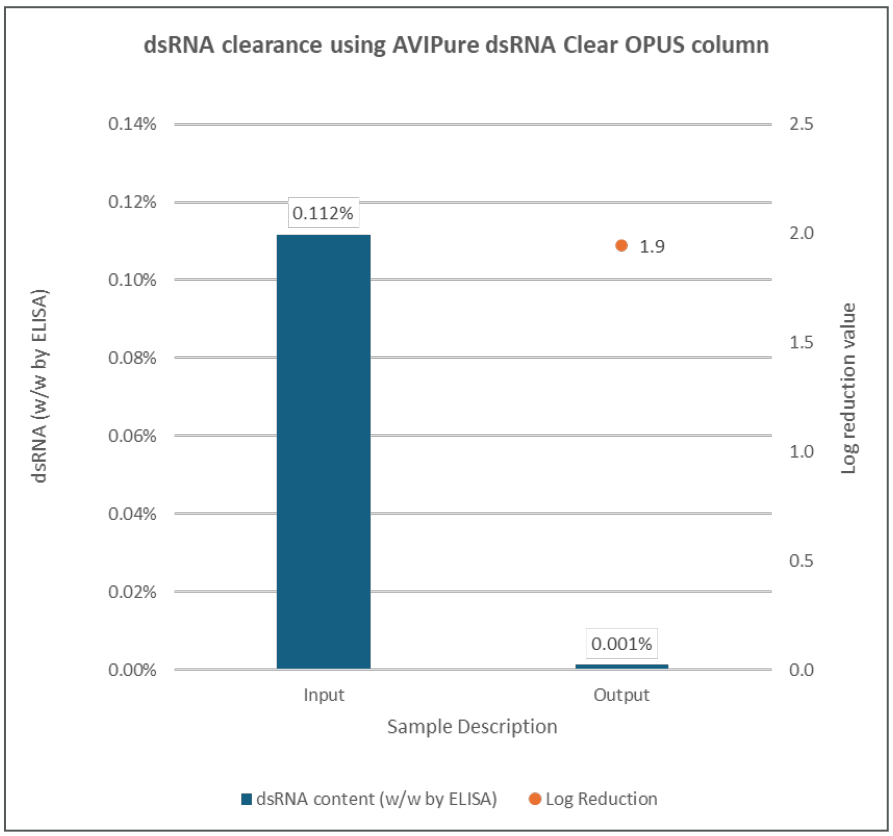

Click here to learn more

repligen.com

REPLIGEN

NUCLEIC ACID INSIGHTS

Meet the

Nucleic Acids Insights Editorial Board

What are your top predictions for the next five years in the nucleic acids field?

An integral part of the team that brings you *Nucleic Acid Insights* is our fantastic Editorial Advisory Board. This article is part of our 'Meet the EAB' series, created to showcase the leaders in the field who provide their time and expertise to help to steer the scope and focus of the journal. Here, members of our board share their top predictions for the field in the coming years.

Nucleic Acid Insights 2025; 2(6), 99–101 · DOI: 10.18609/nuc.2025.015

Jian Yan, Vice President, Research and Discovery, Geneos Therapeutics

I expect major breakthroughs in nucleic acids-based cancer vaccine development. Probably, we will see a few approvals of nucleic acid therapies to either prevent disease recurrence or treat cancer patients.

Piotr Kowalski, Associate Professor in Advanced Therapies, School of Pharmacy, University College Cork, and a Funded Investigator at APC Microbiome Ireland

I hope to see improvements in our understanding of nanoparticle organ tropism (protein corona formation), machine learning for formulation/biomaterial development, engineering novel synthetic RNA payloads (circRNAs, saRNAs), and oral delivery of RNA payloads. I also predict a resurgence of targeted nanoparticles (first clinical approval of targeted RNA/CRISPR LNP formulation), and to see novel types of non-viral delivery systems (non-ionizable-lipid based). Finally, I hope to see positive data from the first *in vivo* CAR-T clinical trials.

Jim Weterings, VP, Head of Oligonucleotide Therapeutics,
Bonito Biosciences

I have two predictions: we will see progress with bispecific siRNAs in the liver and CNS, and the success of siRNA programs in lung.

Myriam Mendila, Chief Development Officer,
CureVac

I think that in the near future we will see a breakthrough in cancer vaccines as well as in prophylactic vaccines targeting so far untargetable pathogens (e.g., bacterial/fungal pathogens) with high unmet need. Given the efforts and progress in delivery of RNA based therapeutics, I also expect rapid progress in organ-targeted delivery of RNA therapies which will open new frontiers for medical applications of RNA technologies in other therapeutic areas such as, for example, autoimmune diseases or other diseases requiring more local reach of RNA therapeutics (ophtha/mucosa etc.) .

David Salzman, Chief Executive Officer,
Gatehouse Bio

Over the next five years, I believe the nucleic acid field will continue to be one of the fastest growing areas in healthcare and that growth will accelerate across multiple sectors including:

- AI-powered target discovery and drug design;
- advancements in conjugates and lipid nanoparticles for tissue and cell-specific oligonucleotide delivery; and
- improvements in oligonucleotide manufacturing that improve yield and lower racemic mixes.

John Counsell, Associate Professor,
University College London

I predict we'll see genAI incorporation into DNA and mRNA coding designs. Improved *de novo* DNA synthesis capabilities will emerge, accelerating access to materials for R&D. More approvals of nucleic acid therapeutics will clear the regulatory pathway for future products. Improved nonviral DNA delivery systems will emerge, addressing a challenging unmet technological need.

Yupeng Chen, Associate Professor at the University of Connecticut and Co-Founder of Eascra Biotech

I expect significant advancements in mRNA and gene editing therapies, along with a surge in new delivery technologies designed to target hard-to-reach tissues.

Veikko Linko, Associate Professor, University of Tartu, Estonia and Visiting Professor, Aalto University, Finland

Many researchers who have been working with DNA nanostructures in our field are now increasingly focusing on similar fully RNA-based or hybrid RNA/DNA nano-objects. Therefore, I believe there might be also some developments within the following areas:

- more (and more precise) CRISPR/Cas -based genome editing using DNA/RNA nanostructures;
- new mRNA delivery vehicles/systems;
- DNA/RNA nanostructure-based cancer immunotherapies/vaccine development; and
- tackling antimicrobial resistance (AMR) using nucleic acids.